Technical Report ITL-95-8
September 1995

US Army Corps of Engineers
Waterways Experiment Station

Computer-Aided Structural Engineering (CASE) Project

Constitutive Modeling of Concrete for Massive Concrete Structures, A Simplified Overview

by Kevin Z. Truman, Washington University
Barry D. Fehl, WES

Approved For Public Release; Distribution Is Unlimited

Prepared for Headquarters, U.S. Army Corps of Engineers

Computer-Aided Structural Engineering (CASE) Project

Technical Report ITL-95-8
September 1995

Constitutive Modeling of Concrete for Massive Concrete Structures, A Simplified Overview

by Kevin Z. Truman

Washington University
Department of Civil Engineering
One Brookings Drive
St. Louis, MO 63130

Barry D. Fehl

U.S. Army Corps of Engineers
Waterways Experiment Station
3909 Halls Ferry Road
Vicksburg, MS 39180-6199

Final report

Approved for public release; distribution is unlimited

Prepared for U.S. Army Corps of Engineers
Washington, DC 20314-1000

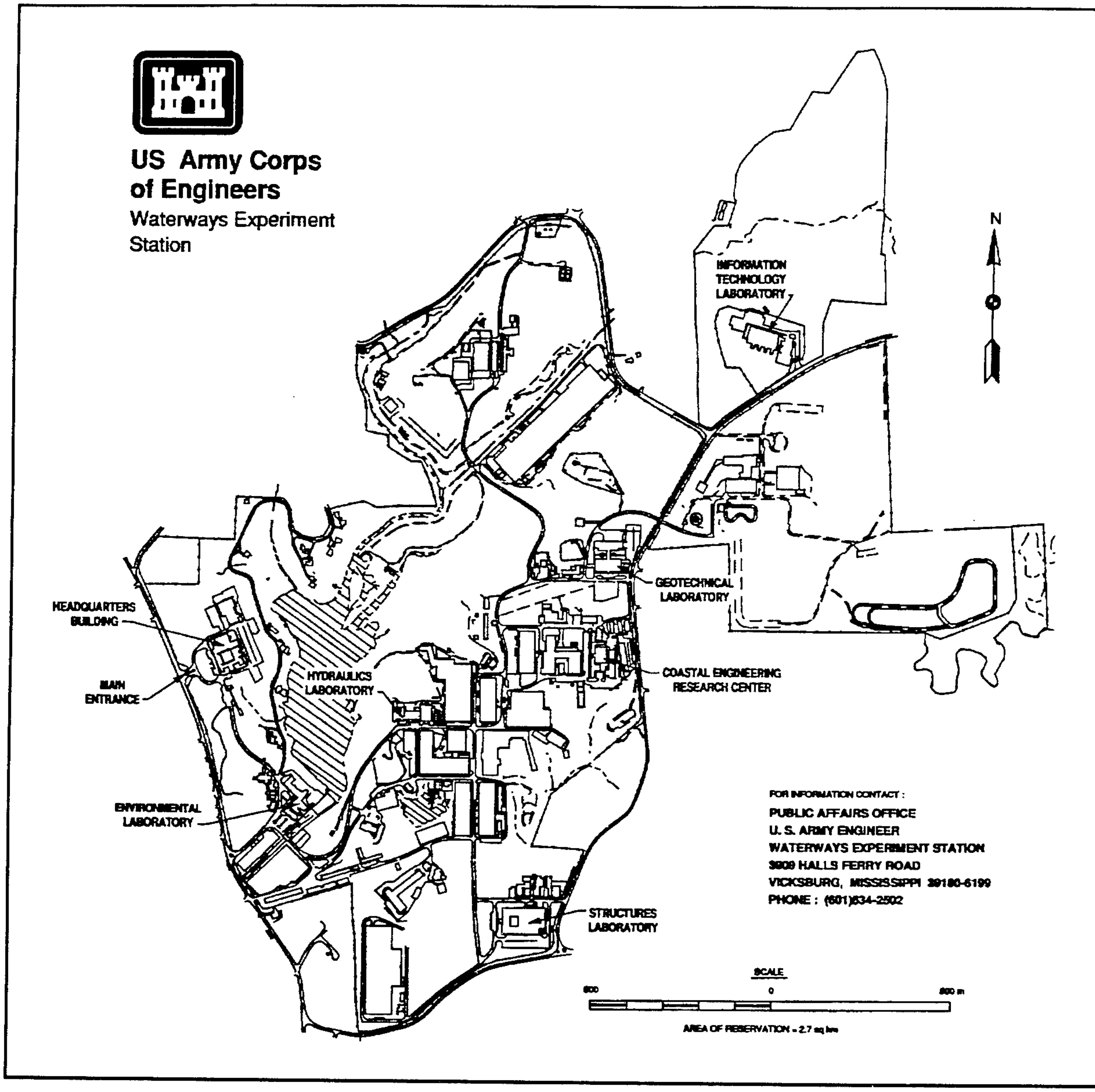

Waterways Experiment Station Cataloging-in-Publication Data

Truman, Kevin Z.

Constitutive modeling of concrete for massive concrete structures : a simplified overview / by Kevin Z. Truman, Barry D. Fehl ; prepared for U.S. Army Corps of Engineers.

65 p. : ill. ; 28 cm. — (Technical report ; ITL-95-8)

Includes bibliographic references.

1. Concrete construction — Mathematical models. 2. Structural analysis (Engineering) I. Fehl, Barry D. II. United States. Army. Corps of Engineers. III. U.S. Army Engineer Waterways Experiment Station. IV. Information Technology Laboratory (U.S. Army Engineer Waterways Experiment Station) V. Computer-aided Structural Engineering Project. VI. Title. VII. Series: Technical report (U.S. Army Engineer Waterways Experiment Station) ; ITL-95-8.

TA7 W34 no.ITL-95-8

Contents

List of Figures

Preface

This report was written to provide the practicing engineer with a document in easy to understand terms and format explaining the constitutive model used in a nonlinear, incremental structural analysis (NISA). The work was sponsored under funds provided to the U.S. Army Engineer Waterways Experiment Station (WES) by the Engineering Division of Headquarters, U.S. Army Corps of Engineers (HQUSACE), as part of the Computer-Aided Structural Engineering (CASE) Project.

The report was compiled and written by Dr. Kevin Z. Truman, Washington University, and Mr. Barry D. Fehl, Information Technology Laboratory (ITL), WES. The work was managed, coordinated, and monitored in the ITL, by Mr. Fehl, Computer-Aided Engineering Division (CAED), under the general supervision of Mr. H. Wayne Jones, Chief, CAED, and Dr. N. Radhakrishnan, Director, ITL.

At the time of publication of this report, Director of WES was Dr. Robert W. Whalin. Commander was COL Bruce K. Howard, EN.

Conversion Factors, Non-SI to SI Units of Measurement

Non-SI units of measurement used in this report can be converted to SI units as follows:

Multiply	By	To Obtain
inches	0.254	meters
pounds per square inch (psi)	6,894.757	pascals

1 Introduction

In order to perform a nonlinear, incremental structural analysis (NISA) on a massive concrete structure such as a lock monolith, gravity dam, or arch dam, the structure's material behavior must be accurately modeled. This behavior is modeled through the use of a set of constitutive relationships that interact to define the material properties as a function of stress, strain, temperature, and age to be used in the analysis to predict the structural response to a given load history. The state-dependent material properties are developed for a specific time in the history of the structure being analyzed and are used to predict the new state of the structure material's behavior at the end of the specific time step.

ANATECH Model

When performing a NISA as defined within ETL 1110-2-365 (31 August 1994) requires the investigator (user) to provide a constitutive model for the material. In order to implement a specialized constitutive model, a general purpose finite element program such as ABAQUS with a user-defined material subroutine (called UMAT in ABAQUS) is required. ANATECH Research Corp. has developed a user-defined constitutive model for several different applications including one for mass concrete systems (ANATECH 1992). These constitutive models have been incorporated into a software package called ANACAP-U that has been developed specifically for use with the program ABAQUS.

Purpose of This Report

Engineers without the proper background or expertise would find the development of a material modeling subroutine extremely difficult if not impossible. Therefore, this report's purpose is to discuss and define the components of the constitutive model to be used within a NISA in a direct and simplified manner. This simplified discussion should provide enough technical information coupled with practical descriptions to yield a general understanding of modeling material behavior.

Currently, the constitutive model defined in ETL 1110-2-365 to be used in a NISA is required to model the concrete's modulus, its creep compliance, its autogenous shrinkage characteristics, and its cracking potential. Each of these properties is dependent on several but not all of the following parameters: age, ambient conditions, internal temperature distribution, time, stress state, strain state, loading, and concrete mixture design or concrete constituents. Each of these components will be discussed in a technical yet practical manner.

Purpose of Model

The purpose of the constitutive model is to accurately model the concrete material's behavior during incremental construction and its service life in order to analyze the structure's state of stress and strain. For this to occur, the strain must be broken into components that reflect the thermal, creep, shrinkage, and mechanical strains. The accuracy of these four material-related components are totally dependent upon the constitutive model and its relation to the true (experimental) behavior of the actual material used in construction. The strain within a massive concrete structure is three dimensional and can be broken into four components as

$$\tilde{\varepsilon} = \tilde{\varepsilon}^m + \tilde{\varepsilon}^T + \tilde{\varepsilon}^s + \tilde{\varepsilon}^c \qquad (1)$$

where

ε^m = mechanical strain (elastic and plastic)

ε^T = thermal-induced strains

ε^s = shrinkage strains

ε^c = creep-related strains

Given a state of stress and strain at the beginning of an increment and the incremental total strain $\Delta\varepsilon$, the constitutive model must compute the state of stress σ and, for implicit calculations, the material tangent stiffness matrix (i.e., the Jacobian of the constitutive law $\partial\Delta\sigma/\partial\Delta\varepsilon^m$) at the end of the increment. The stress and "tangent" constitutive matrix must be compatible with the failure and loading surfaces of the material such as cracking in tension and yielding in compression. Since a constitutive law relates stresses to mechanical strains, the thermal, shrinkage, and creep strains must be removed from the given total strains and strain increments by the model before defining the stresses. ANATECH Research Corp. has developed such a model for use in the ABAQUS general purpose finite element code.

2 Creep

After concrete is loaded it begins to deform continually with time. This deformation has two components: the first is the mechanical deformation which is immediate and the second is time dependent and can continue for years. This second component of deformation is referred to as creep. Creep is commonly defined as the dimensional change or increase in strain (elongation or shortening) with time due to a sustained stress. Creep can be beneficial or detrimental to a structure. Depending on the structural configuration, creep can cause excessive deformation at later times, but it can also relieve stresses at locations of stress concentrations by redistributing the stresses. For structures with sustained thermal gradients, creep can reduce the initial thermal stresses, but it can also produce stress reversals once the structure has cooled (Fintel 1974).

Specific creep is defined as the creep strain per unit of sustained stress. The ultimate specific creep usually ranges from 0.2 to 2.0 millionths per psi.[1] Very-early-age deformation due to creep is viscoplastic in nature and predominantly unrecoverable, whereas deformation due to creep in older concrete tends to be viscoelastic and predominantly recoverable. The lack of creep strain recovery in very young concrete is primarily due to the rapidly aging modulus, which gives the material an apparent viscoplastic behavior. However, in mature concrete aging is small and creep strain recovery is almost total given sufficient time.

Controlling creep is a formidable task since it is a function of the concrete constituents, the concrete's age at the time of loading, the dimensions of the structure, ambient conditions, and curing procedures. Constituents that affect creep include the water-cement ratio, aggregate size, aggregate type, and cement paste characteristics. If only the cement paste constituents are considered, the higher the rate of strength gain, the lower the creep deformation for a given stress. Therefore, an important parameter in creep prediction is the ratio of applied stress to the strength at the time of loading. Creep is generally a linear function of the stress-strength ratio up to 50 percent of the concrete's ultimate strength at which point the creep becomes nonlinear. The aggregates

[1] A table of factors for converting non-SI units of measurement to SI units is presented on page vi.

affect creep by providing restraint with respect to creep deformation of the cement paste. A larger volume of aggregate generally produces a larger reduction in creep deformation. (This action also depends on the physical properties of the aggregate such as the modulus of elasticity, porosity, grading, and bondability.) Creep is temperature dependent. The creep strain can increase for some concrete mixtures for temperatures between 70 and 100 °F (Fintel 1974).

Loading rate has a significant effect on the creep. For a step load, the rate of creep will be relatively high during the first few days of loading, but will eventually approach zero after some finite amount of time. The age of loading has a significant effect on the creep-dependent deformations. Early-age-loaded concretes will have much larger ultimate specific creep than a specimen loaded at a later age due to the fact that specific rate decreases as the strength-to-stress ratio increases at the time of loading. Figure 1 shows the total (elastic

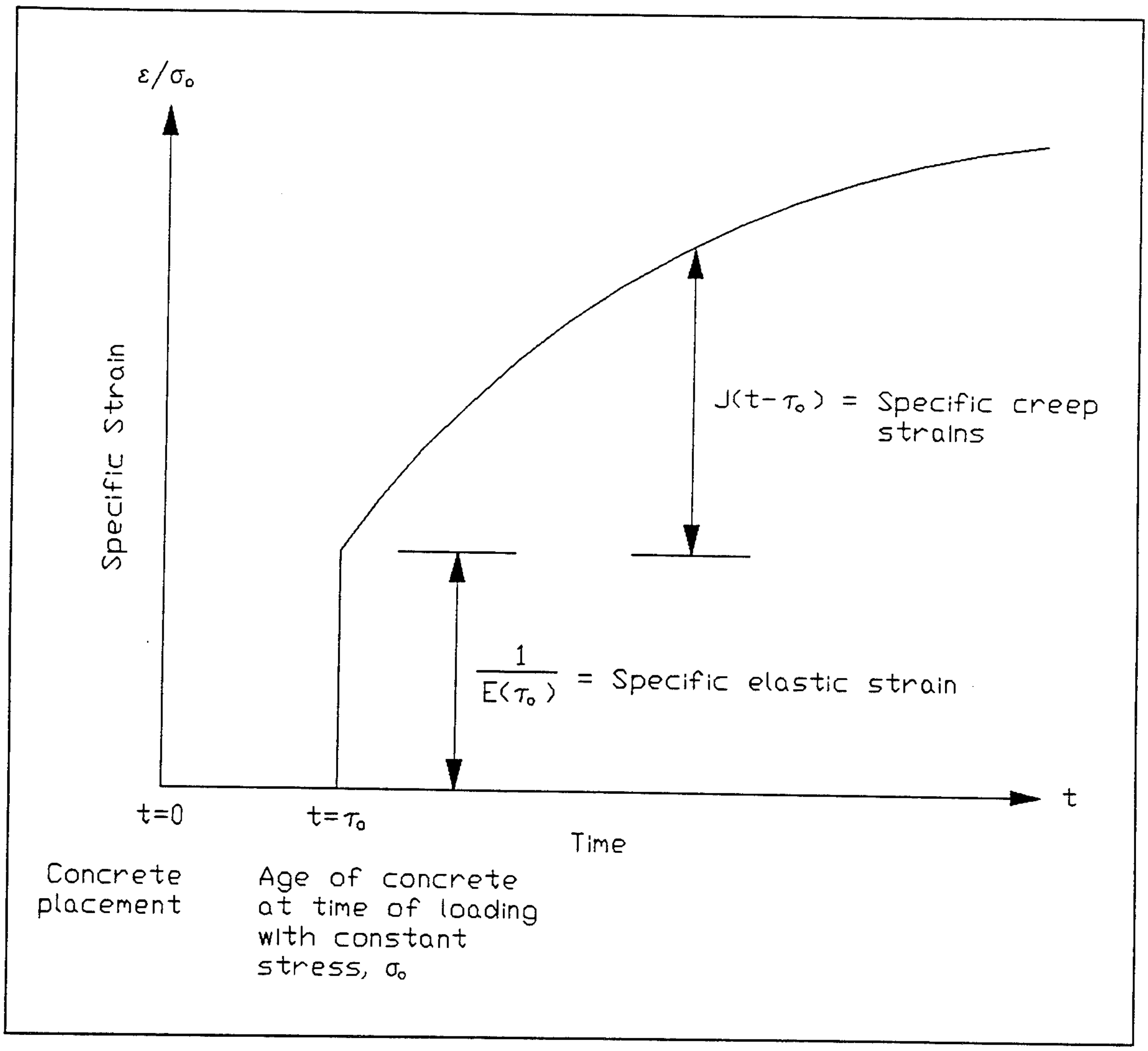

Figure 1. A generalized specific strain curve for concrete

and creep) specific strain as a function of time and loading age. The elastic portion of the curve (denoted as specific elastic strain in Figure 1) is the inverse of the aging modulus. The curve above the elastic response is the apparent creep curve which is greatly influenced by the age at loading. (See discussion below for the definition of apparent creep versus true creep.)

Figure 2 gives typical experimental curves for a concrete cylinder that shows the dependence of specific strain on the age of the concrete at the time of loading. These experimentally developed compliance curves (specific

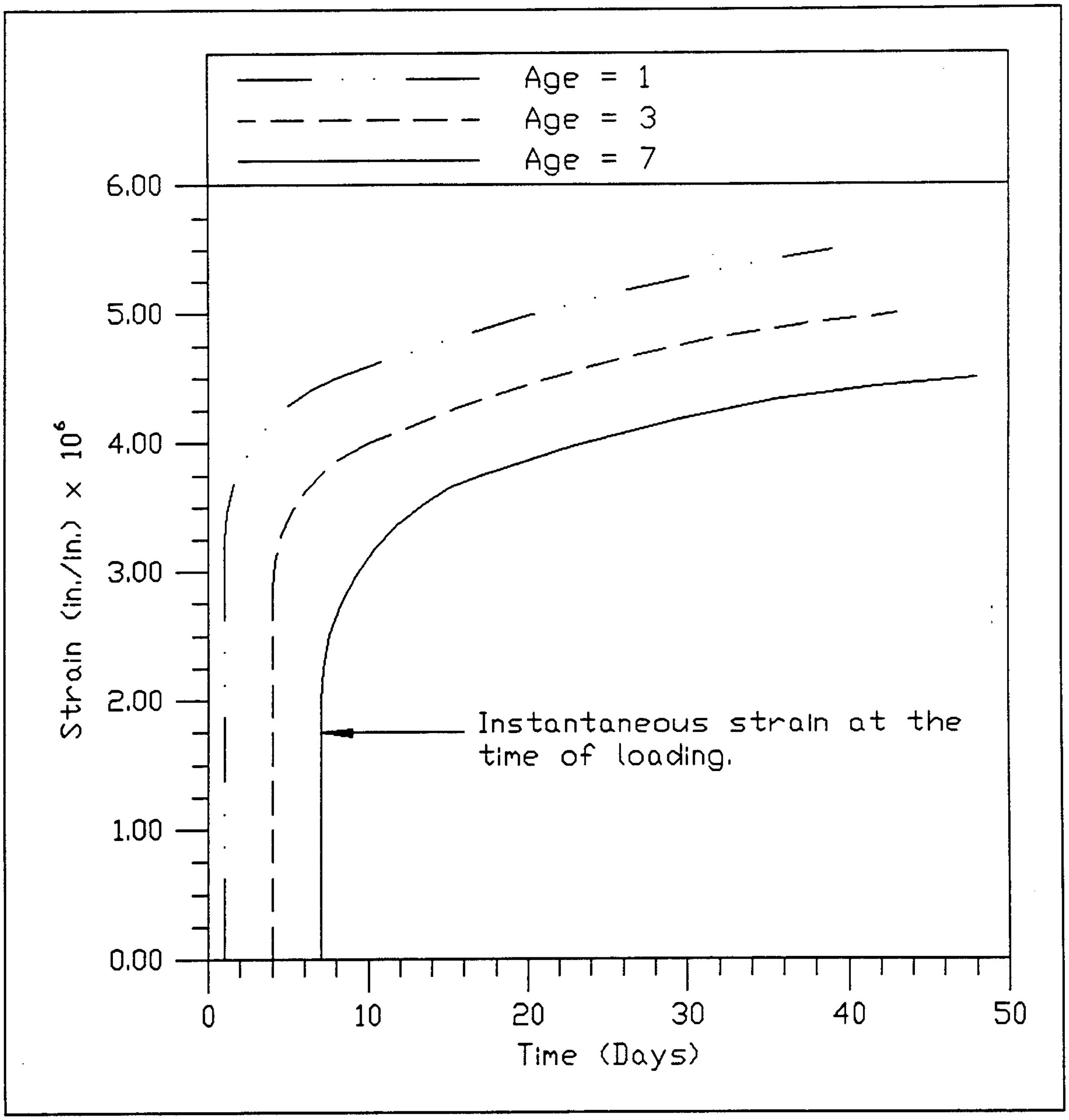

Figure 2. Experimentally derived creep strain curves for concrete cylinders

strain) are composed of two distinct components. The first data point on each of the curves represents the elastic specific strain component. The second component is the time curve which represents the apparent creep. The older the concrete, the lower the values of the elastic and creep strains.

Figure 3 is a generalized specific creep curve for concrete loaded with a uniaxial stress of σ_0 at age τ_0 and can be used to show the effects of aging in concrete compliance. The first component is the elastic specific strain, ε^e/σ_0, represented by the vertical portion of the curve. This specific elastic strain can be denoted as the inverse of the elastic modulus at age τ_0, $1/E(\tau_0)$. At age τ_n the concrete has been unloaded, thereby causing a reduction in the specific strain of $1/E(\tau_n)$. As seen in Figure 3, $J(t-\tau_0)$ is the measured data using the initial specific elastic strain as the reference datum. Hence, $J(t-\tau_0)$ is called the apparent creep compliance. In reality as the concrete ages to τ_n, the true specific creep strain or creep compliance should be $C(t-\tau_0, \tau_n)$ which reflects the changing modulus. Therefore, the total specific strain can be written in either of two forms:

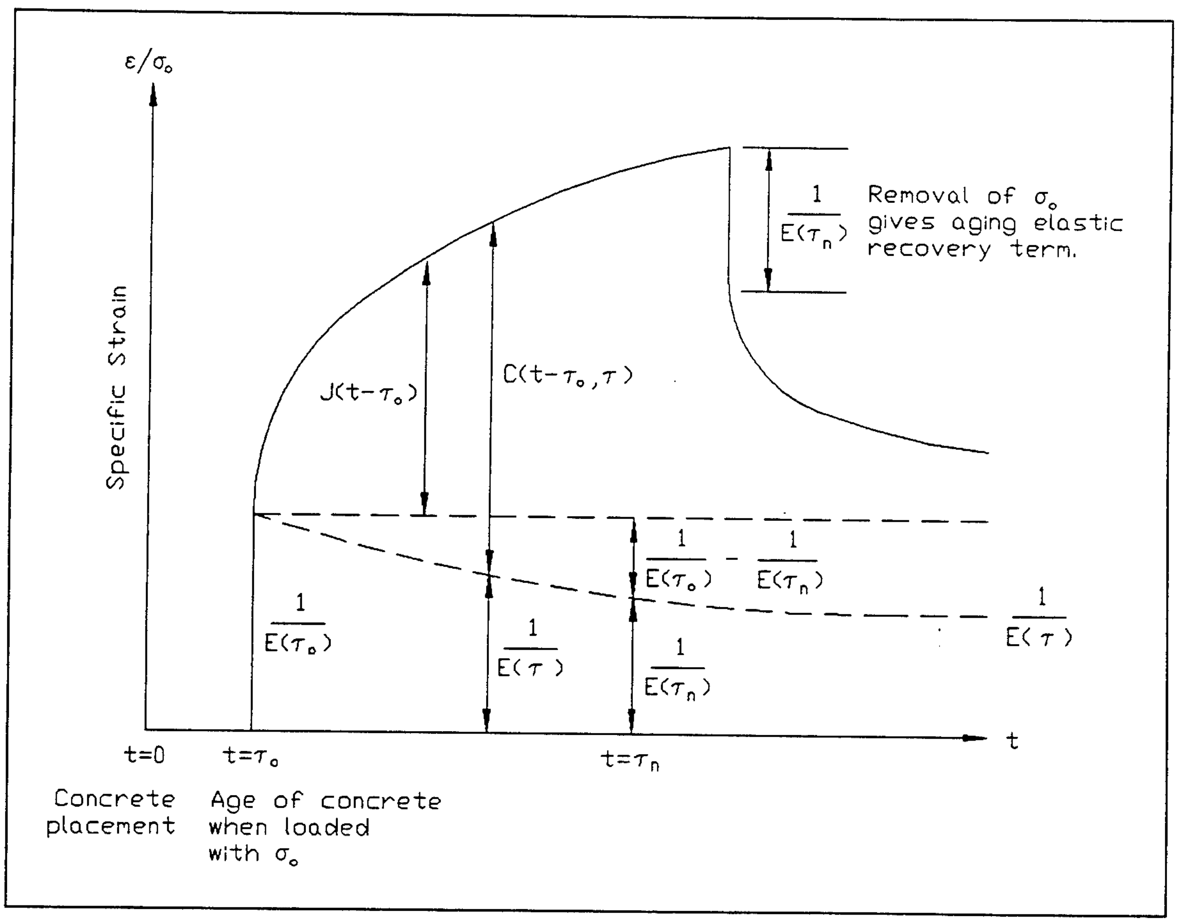

Figure 3. Compliance curve for concrete

$$\frac{\varepsilon}{\sigma} = \frac{1}{E(\tau_0)} + J(t - \tau_0) = \frac{1}{E(\tau_n)} + C(t - \tau_0, \tau_n) \tag{2}$$

which can be rearranged to give the true creep compliance as:

$$C(t - \tau_0, \tau_n) = \left[\frac{1}{E(\tau_0)} - \frac{1}{E(\tau_n)}\right] + J(t - \tau_0) \tag{3}$$

For nonaging materials, $E(\tau_0) = E(\tau_n)$, and in that case Equation 3 shows that J and C would be equivalent. If the concrete is mature prior to loading, E becomes nearly constant and J and C are nearly equivalent as shown in Figure 4 for $t = \tau_3$. For early-age loading, J and C can be quite different depend ing on the constituents of the concrete. Quite often the experimentally derived data for J are used as the creep compliance term causing some error in the predicted versus the experimental data. This error is due to the aging modulus and is the difference between $1/E(\tau_0)$ and $1/E(\tau_n)$ as seen in Figure 3 and Equation 3. For modeling purposes separate identification of the curves C and J is not necessarily required. What is required is a model which adequately represents the experimental behavior in loading and unloading requiring the experimentally derived specific strain curve and an accurate aging modulus model.

Creep compliance (specific strain beyond the elastic specific strain) has been modeled by ANATECH in a computer subroutine as a single equation which is dependent upon time t, age τ, and temperature T. The equation is of the form:

$$J(t,\tau,T) = \sum_{i=1}^{2} A_i(\tau,T)\left(1 - e^{-r_i(t-\tau)}\right) + D(\tau,T) * (t - \tau) \tag{4}$$

where

$$A_i(\tau,T) = A_{ci}\, e^{-Q/RT}\left[\frac{E(\tau_0)}{E(\tau)}\right]^p \tag{5}$$

and

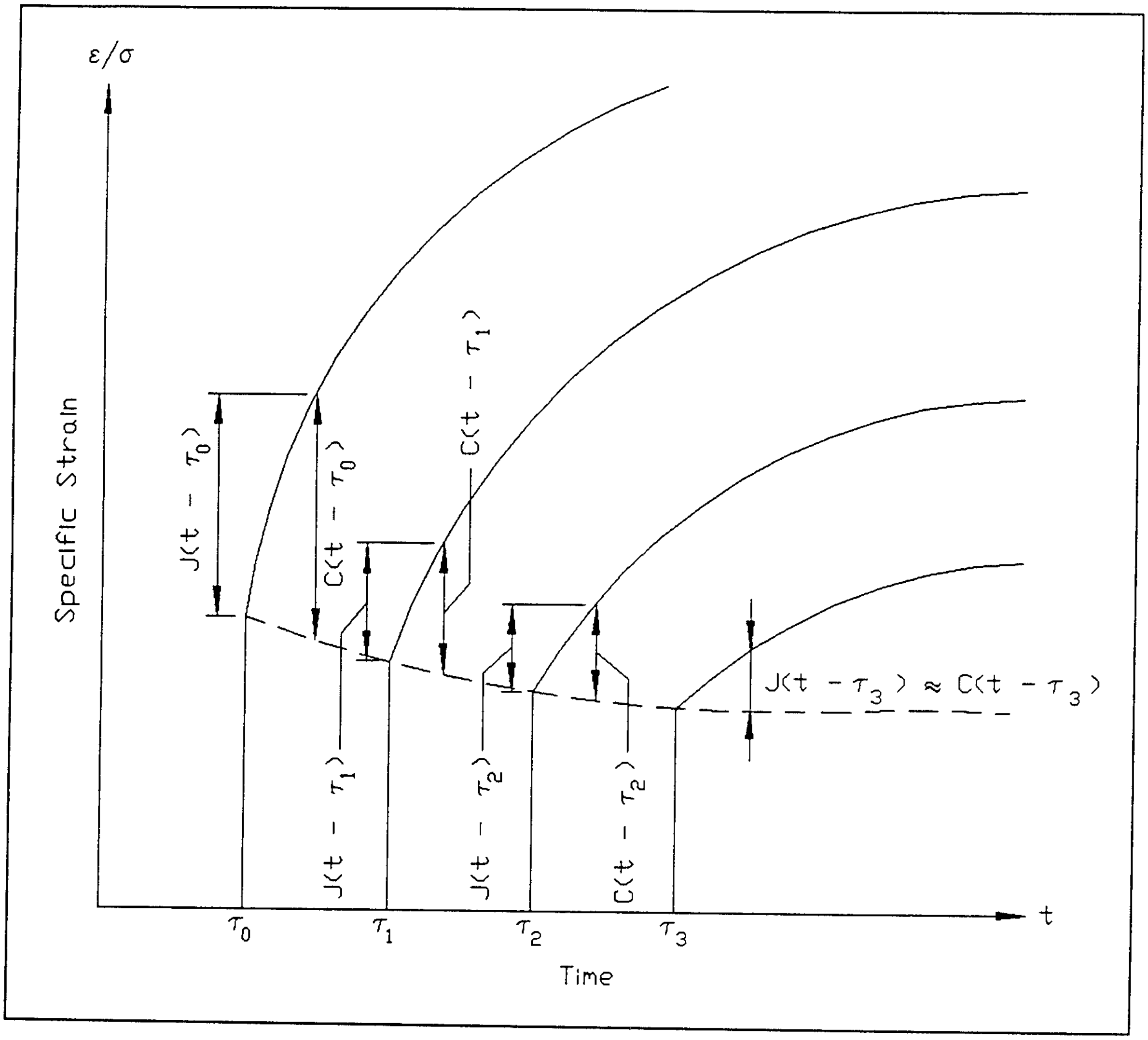

Figure 4. Concrete compliance curves at different ages of loading

$$D(\tau,T) = D_c e^{-Q/RT} \left[\frac{E(\tau_0)}{E(\tau)} \right]^p \tag{6}$$

where

R = universal gas constant of 1.98

A_1, A_2, r_1, r_2, p, Q, and D = mathematically derived constants using experimental data

τ_0 = reference age at which creep specimen is loaded

These equations can be used to represent the experimental results by determining the appropriate values for the constants A_1, A_2, r_1, r_2, and D. The experimentally derived constants required for this equation ensure a consistent match between the experimental data and the computerized constitutive model. The constants are determined using this procedure:

Step 1. Select an experimental creep curve for a given age τ_0, 3-day creep is a common age for early creep experiments.

Step 2. Select three times representing early, intermediate, and long-term values in order to obtain an adequate curve fit for each region. Assume 4, 31, and 93 days.

Step 3. Assume $e^{-r_1(4-3)}$ to be a small value, 0.001 to 0.005, which will cause the first term $(1 - e^{-r_1(4-3)})$ to be dominant at early times. Solve for r_1 (i.e., $e^{-r_1(4-3)} = 0.001 \Rightarrow r_1 = 6.908$).

Step 4. Assume $e^{-r_2(31-3)}$ to be a small value, 0.001 to 0.005, which will cause the second term to be dominant in the intermediate range. Solve for r_2 (i.e., $e^{-r_2(31-3)} = 0.001 \Rightarrow r_2 = 0.247$).

Step 5. Select three values for $(t-\tau)$, continue to use $\tau = 3$ days and the 3-day experimental creep curve and find the appropriate experimental creep compliance values. Construct these three equations:

$$J(t_1,3) = A_1\left(1 - e^{-r_1(t_1 - 3)}\right) + A_2\left(1 - e^{-r_2(t_1 - 3)}\right) + D * (t_1 - 3) \quad (7)$$

$$J(t_2,3) = A_1\left(1 - e^{-r_1(t_2 - 3)}\right) + A_2\left(1 - e^{-r_2(t_2 - 3)}\right) + D * (t_2 - 3) \quad (8)$$

$$J(t_3,3) = A_1\left(1 - e^{-r_1(t_3 - 3)}\right) + A_2\left(1 - e^{-r_2(t_3 - 3)}\right) + D * (t_3 - 3) \quad (9)$$

and solve for A_1, A_2, and D. It should be noted that because of the linear term in Equation 4, the creep rate at long time approaches a constant value instead of zero, which strictly is not true. However, the error is small, and on the conservative side, for load durations of interest. This situation can be corrected by replacing the linear term by another exponential term where

r_3 would be found using Steps 3 and 4 and A_3 would be determined in Step 5. Steps 6-11 need only be performed if T is considered as a variable.

Step 6. Select a reference temperature T_0 and another temperature $T > T_0$ (Kelvin).

Step 7. Determine the creep compliance values for a fixed time t and age τ (31 and 3 days, respectively, are reasonable values) from experimental creep data for temperatures T_0 and T.

Step 8. Construct this equation:

$$\frac{e^{-Q/RT}}{e^{-Q/RT_0}} = e^{\frac{-Q}{R}\left(1/T - 1/T_0\right)} = \frac{J\left(31,3,T\right)}{J\left(31,3,T_0\right)} \tag{10}$$

Solve for Q.

Step 9. If experimental creep data are available for a third temperature T_3, calculate the specific creep strain $J(31,3,T_3)$ from the fully defined equation and compare with the experimental creep data for the chosen time, age, and temperature (31, 3, T_3, respectively).

Step 10. If the error is large, adjust Q in a manner which will reduce the error. Repeat until the error is acceptable.

Step 11. Check for other values of t, τ, and T_3. Adjust Q until there is convergence or the error is within an acceptable accuracy.

After the steps outlined above are performed, the resulting effect of the constants computed must be determined by performing analyses of a single element using the loading that was applied in the laboratory for 1-, 3- and 14-day creep tests. The resulting strains of these analyses should be compared directly with the strain data obtained in the laboratory. If the results of all three analyses do not compare well with the test data then the constants must be adjusted, the analyses performed, and once again the results compared with the test data. This iterative process must continue until a satisfactory comparison of all three strain tests is achieved. The process used in adjusting the constants is demonstrated in Appendix A.

Figure 4 shows different creep compliance curves for concrete loaded at various ages. Concrete loaded at age τ_0 has a different compliance curve than a concrete loaded at age τ_1. The assumption that the reduction in the rate of creep with increasing age is proportional to the increase in the modulus with increasing age provides the reasoning for the use of a ratio of the modulus at different ages to adjust the creep compliance curve for aging. With a reference age of 3 days, the ratio becomes $E(3)/E(\tau)$. Figure 5 shows creep compliance

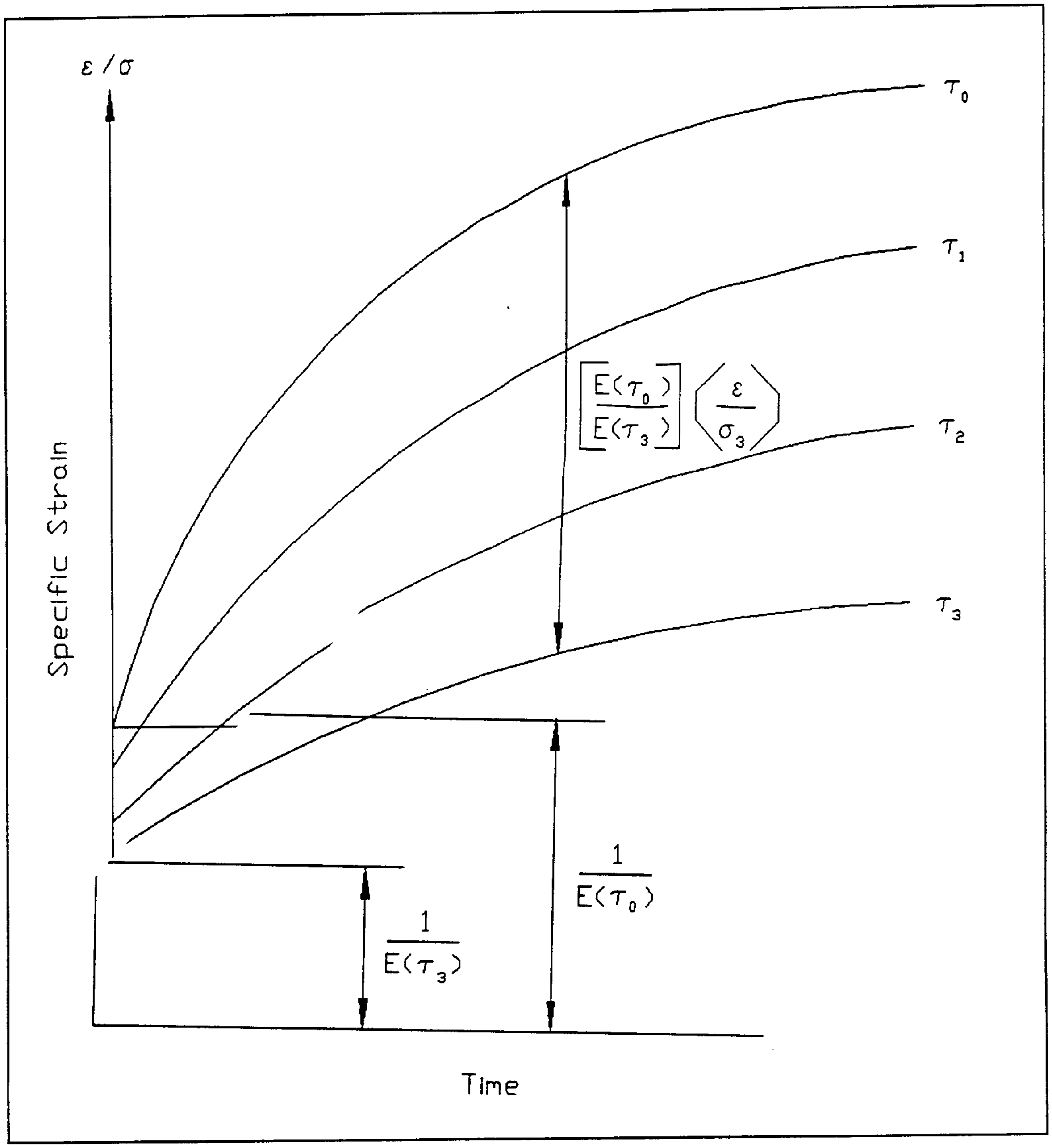

Figure 5. Concrete compliance curves as a function of duration of loading

as a function of load duration, $t - \tau$. For equal durations of load, it is shown that early loading produces significantly more creep-related strain than a late-age loading. The ratio of the concrete compliance curve values at a specific duration of loading is the true adjustment factor. From experimental data it has been determined that the aging effects are best represented with a factor of $[E(3)/E(\tau)]^p$ where p is between one and two. As seen in Equations 5 and 6, this factor is used to account for the aging effects in the creep equation. The value for p can be experimentally determined.

Concrete creep is assumed to follow a thermo-rheologically simple behavior which allows the creep curve at any temperature T to be generated from a reference creep curve developed for temperature T_0 (reference). This type of behavior implies that a creep curve at any temperature when plotted as a function of log t can be obtained by a simple shift of the reference curve along the log t axis. The shift $\phi(T)$ is called a shift factor and the log of $\phi(T)$ is called the shift function. This behavior allows the implementation of an extrapolation scheme that can cover a wide range of temperatures with only a few temperature-controlled creep tests. Equation 9 can be rewritten to adjust for temperature effects in creep compliance as:

$$J(t,\tau,T) = J(t,\tau,T_0)\frac{e^{-Q/RT}}{e^{-Q/RT_0}} \qquad (11)$$

The factor for adjusting the creep compliance for temperature effects in the ANACAP-U subroutine becomes:

$$\Phi(T) = e^{-Q/RT} \qquad (12)$$

since the terms related to T_0 are already coupled in the experimental data used to generate the creep compliance constants A_1, A_2, r_1, r_2, and D. Once again if temperature is found to be of little or no importance the use of thermal adjustment factors is unnecessary.

3 Autogenous Shrinkage

Autogenous shrinkage is a decrease in volume of a concrete specimen or member due to hydration of the cementitious materials without gaining or losing moisture. This type of shrinkage occurs within the central regions of mass concrete systems. For mass concrete systems this component of shrinkage can be significant compared to drying shrinkage. Autogenous shrinkage occurs over a much longer time period than drying shrinkage which is a localized phenomenon that affects only a thin layer of concrete near the concrete ambient air interface. Autogenous shrinkage increases with respect to higher cement content and increased temperatures. Sealed creep cylinders with no external loading have been successfully used as a means of measuring autogenous shrinkage.

The autogenous shrinkage has been modeled by ANATECH in a computer subroutine as a single equation with four required constants and two time-dependent exponential terms:

$$\varepsilon_s(t) = C_1\left(1 - e^{-s_1 t}\right) + C_2\left(1 - e^{-s_2 t}\right) \qquad (13)$$

These constants are evaluated in a manner similar to that for the creep constants.

Step 1. Select a late time t (100 to 300 days). Assume that the term $e^{-s_2(100)}$ is small (0.001 to 0.005). Solve for s_2 (i.e. $e^{-s_2(100)} = 0.001 \Rightarrow s_2 = 0.0691$).

Step 2. Select an intermediate time t (20 to 60 days). Assume that the term $e^{-s_1(40)}$ is small (0.001 to 0.005). Solve for s_1 (i.e., $e^{-s_1(40)} = 0.001 \Rightarrow s_1 = 0.1727$).

Step 3. Select two data points from the experimental data $\varepsilon_s(30)$ and $\varepsilon_s(100)$. Substitute these values into Equation 13.

$$\varepsilon_s(100) = C_1\left(1 - e^{-s_1(100)}\right) + C_2\left(1 - e^{-s_2(100)}\right) \qquad (14)$$

$$\varepsilon_s(30) = C_1\left(1 - e^{-s_1(30)}\right) + C_2\left(1 - e^{-s_2(30)}\right) \tag{15}$$

Step 4. Solve the equations for the constants C_1 and C_2.

Step 5. Once the constants have been determined, the equation using these constants should be compared with the experimental data in order to explore the accuracy of the generated curve. Adjust s_1 and s_2 until a satisfactory curve is generated.

4 Aging Modulus

The modulus of elasticity for concrete is generally defined from compressive tests. It is heavily dependent upon the cement paste, aggregate modulus of elasticity, and the relative volumes of aggregate to cement paste. The dependence of modulus of elasticity on the cement paste is the reason that the modulus is also concrete-age dependent. The cement paste modulus is dependent upon the amount of hydration that has occurred, increasing as the hydration process continues. Also the increased bonding of the cement paste to the aggregate improves the composite action of the cement paste and aggregate which is also a function of the hydration or curing of the concrete. Typically, the modulus of elasticity increases faster than the compressive strengths at early ages (Fintel 1974).

The aging modulus as a function of concrete age has been modeled in the ANATECH version of UMAT (ANACAP-U) by a single equation. Within this equation several constants must be determined in order to fit the curve to the experimental aging modulus data. The equation is of the form:

$$E(\tau) = E_0 + E_1\left(1 - e^{-c_1(\tau - 1)}\right) + E_2\left(1 - e^{-c_2(\tau - 1)}\right) + E_3\tau \qquad (16)$$

where τ is the age of the concrete given in days. One way to fit the equation to the actual aging modulus versus age data is to generate four equations to solve for the four constants E_i. Each term in the equation is used to best represent a region of the actual aging modulus data. E_0 is used to represent the first day; E_{1r} is used to represent the data for early values (5 to 10 days); E_2 is used to represent the data for intermediate values (20 to 40 days); and E_3 is used to represent late data. Typically the constants would be determined by this procedure:

Step 1. E_0 is the value of the aging modulus at $\tau = 1$ day. Any value of the aging modulus required prior to $\tau = 1$ day is determined using linear interpolation from 0 to the value for day 1.

Step 2. Select an intermediate age such as 28 days where aging effects are small or can be neglected. Assume the term $e^{-c_1(28-1)}$ is small (0.001 to 0.005). Solve for c_1 (i.e., $e^{-c_1(28-1)} = 0.001 \Rightarrow c_1 = 0.2558$).

Step 3. Select an early age such as 7 days where the intermediate age effects are small or can be neglected. Assume the term $e^{-c_2(7-1)}$ is small (0.001 to 0.005). Solve for c_2 (i.e., $e^{-c_2(7-1)} = 0.001 \Rightarrow c_2 = 1.151$).

Step 4. Determine the experimental values for $E(7)$, $E(28)$, and E(90 days or later) from the experimental data. The values of 7 and 28 days are usually convenient since many experiments are developed to collect data at those two concrete ages.

Step 5. Solve the corresponding four equations for E_i, $i = 0...3$.

$$E(1) = E_0 \tag{17}$$

$$E(7) = E_0 + E_1\left(1 - e^{-e_1(7-1)}\right) + E_2\left(1 - e^{-e_2(7-1)}\right) + E_3 * 7 \tag{18}$$

$$E(28) = E_0 + E_1\left(1 - e^{-e_1(28-1)}\right) + E_2\left(1 - e^{-e_2(28-1)}\right) + E_3 * 28 \tag{19}$$

$$E(90) = E_0 + E_1\left(1 - e^{-e_1(90-1)}\right) + E_2\left(1 - e^{-e_2(90-1)}\right) + E_3 * 90 \tag{20}$$

Step 6. Once the six constants have been determined, Equation 16 should be compared with the experimental data in order to explore the accuracy of the generated curve. Adjust the constants to obtain a reasonably accurate equation. Again as in the case of continuously diminishing creep rate at long times, the modulus aging should eventually saturate. Equation 16, however, implies continuous aging approaching a linear rate at long times. If long-term loading is of interest, Equation 16 may have to be refitted with a fourth exponential term instead of a linear term.

5 ABAQUS/ANACAP-U User Material Subroutine

ABAQUS allows the use of a predefined constitutive model through the ABAQUS UMAT subroutine. ABAQUS provides a warning that this option should only be used by experts and that any user-developed constitutive model should be thoroughly tested prior to its implementation. ANATECH's heavy use of ABAQUS and its UMAT subroutine in the analysis of nuclear facilities provided the expertise needed in developing a constitutive model for incrementally constructed massive concrete structures. ANATECH's development of ANACAP-U includes an early-age constitutive model which can be used for massive concrete structures on Corps of Engineers projects.

In order to model the complex behavior of creep, shrinkage, aging modulus, and cracking, a constitutive model subroutine was developed to be used with the ABAQUS finite element code. Nonlinear finite element solutions are highly dependent upon the numerical implementation of a sound constitutive model. The constitutive model's purpose is to accurately define the stresses and the tangent constitutive matrix at the end of each time step. In a finite element program the required equations would be of the form:

$$\Delta\tilde{\varepsilon}^m = \Delta\tilde{\varepsilon} - \Delta\tilde{\varepsilon}^T - \Delta\tilde{\varepsilon}^S - \Delta\tilde{\varepsilon}^C \tag{21}$$

$$\tilde{\sigma}_{t+\Delta t} = \tilde{\sigma}_t + \tilde{D}\Delta\tilde{\varepsilon}^m \tag{22}$$

where

D = the tangent constitutive matrix

$\tilde{\sigma}_i$ = the stresses at time $i = t$ or $t + \Delta t$

$\Delta\tilde{\varepsilon}$ = the difference in the strains at $t + \Delta t$ and t

The increment of total strains $\Delta\tilde{\varepsilon}$ in Equation 21 are those strains that result from the solution of the force-displacement (equilibrium) equations and are returned by ABAQUS to the constitutive subroutine ANACAP-U. The other strain increments $\Delta\tilde{\varepsilon}^i$ due to temperature, shrinkage, and creep are calculated within the constitutive routine. The UMAT subroutine is called by ABAQUS whenever a *MATERIAL definition inside the user input includes a *USER MATERIAL option to define the mechanical constitutive behavior of the material. The *USER MATERIAL option forces every element defined by the *MATERIAL name to be controlled by the UMAT subroutine. The *USER MATERIAL option requires a number that reflects the number of user-defined properties. The properties to be supplied are defined in the ANACAP-U User's Manual (ANATECH Research Corp. 1992) and are presented in Table 1. For further information regarding the property definitions, refer to the ANACAP-U User's Manual.

A portion of the ABAQUS input for the Olmsted Locks NISA is presented in Chapter 6 to illustrate the proper use of the ABAQUS commands and the required input for using the UMAT subroutine as contained in ANACAP-U.

Table 1
Material Properties Required for UMAT Input

Prop. No.	Description	Comments
1	Model Flag =1 Elastic Comp. =2 Elastic Perfectly Plastic Comp. =3 Comp. Strain Hard. and Soft. =4 Elastic Perfectly Plast. Comp. with Creep, Aging and Shrinkage	This flag should be set to 4 for NISA studies
2	Static crushing strength (f_c')	Input f_c' from concrete testing for concrete 3 days old. Typical values are 600 to 1,000 psi
3	Static tensile cracking strain	Calculate using equation from ETL 1110-2-365 and results from slow load beam test performed on selected project mixture
4	Static elastic modulus (E)	Input E from concrete testing for concrete 3 days old. Typical values are 1,500,000 to 2,500,000 psi
5	Poisson's ratio (ν)	Input from concrete testing. Typical values are 0.15 to 0.2
6	Coef. of thermal expansion (α)	Input from concrete testing. Typical values are 4.0×10^{-6} to 6.0×10^{-6} in./in./°F
7	Stress free temp.	Use placing temperature
8	Flag for English or SI Units	Use a 1 for English units
9 to 24	Properties 9 through 24 are not used in a NISA and should all be set to 0.0. Information on these properties can be found in the ANACAP-U User's Manual.	
25	Creep fit flag	Use a value of 2
26	Age of concrete in days	Typically this will be 0.0
27	Shrink factor	Multiplier for shrinkage curve, should be based on bounds being applied to shrinkage as specified in ETL 1110-2-365. If 15% increase is used, factor should be input as 1.15
28	Creep factor	Multiplier for creep curve, should be based on bounds being applied to creep as specified in ETL 1110-2-365. If 15% decrease is used, factor should be input as 0.85
29	Initial shrink. strain	Input as 0.0
30	Reference time	Identifies when the material will begin gaining strength in the analysis (e.g. use 5.0 if material being described is in the 2nd lift and 5.0 day placement intervals are being used)
31	Agg. size parameter	Input as 0.0
32	Reinforcement ratio	Input as 0.0

6 Lock and Dam Constitutive Model Input

The use of ABAQUS or ANACAP-U subroutines is straightforward. A portion of an input file for a NISA of the Olmsted Lock is given below to clarify the required ABAQUS information and commands when using a self-defined constitutive model. The mathematically derived constants that were presented in the chapters regarding creep, autogenous shrinkage, and aging modulus are contained within the constitutive model subroutine and are not input variables. The variables described within Table 1 are typically the variables required within an input file. The ABAQUS commands and Olmsted values for these values are:

*SOLID SECTION, MATERIAL=M1,ELSET=LIF1 *MATERIAL,NAME=M1	Definition for lift No. 1, element set LIF1
*USER MATERIAL, CONSTANTS=32	Identifies material as a user-defined material
4,675.,100.E-6,2.1E6,.15,4.E-6,66.6,1 0.,0.,0.,0.,0.,0.,0.,0. 0.,0.,0.,0.,0.,0.,0.,0. 2,0.4999,1.1,0.9,0.,0.,0.,0.	Input parameters needed for user-defined model as described in Table 1
*DEPVAR 23	Identifies state-dependent variables
*SOLID SECTION, MATERIAL=M2,ELSET=LIF2 *MATERIAL,NAME=M2 *USER MATERIAL,CONSTANTS=32 4,675.,100.E-6,2.1E6,.15,4.E-6,66.6,1 0.,0.,0.,0.,0.,0.,0.,0. 0.,0.,0.,0.,0.,0.,0.,0. 2,0.4999,1.1,0.9,0.,10.,0.,0. *DEPVAR 23	Definition for lift No. 2, element set LIF2
*SOLID SECTION, MATERIAL=M3,ELSET=LIF3 *MATERIAL,NAME=M3 *USER MATERIAL, CONSTANTS=32 4,675.,100.E-6,2.1E6,.15,4.E-6,66.6,1 0.,0.,0.,0.,0.,0.,0.,0. 0.,0.,0.,0.,0.,0.,0.,0. 2,0.4999,1.1,0.9,0.,20.,0.,0. *DEPVAR 23	Definition for lift No. 3, element set LIF3
*SOLID SECTION, MATERIAL=M4,ELSET=LIF4 *MATERIAL,NAME=M4 *USER MATERIAL, CONSTANTS=32 4,675.,100.E-6,2.1E6,.15,4.E-6,66.6,1 0.,0.,0.,0.,0.,0.,0.,0. 0.,0.,0.,0.,0.,0.,0.,0. 2,0.4999,1.1,0.9,0.,30.,0.,0. *DEPVAR 23 . . .	Definition for lift No. 4, element set LIF4

7 Cracking Criteria and Model

A major reason for performing a NISA of a mass concrete structure is to predict the potential for cracking to occur during the construction and service life of the structure. Finding the crack potential within a massive concrete structure provides the designer with important information regarding the quality of the structure. If the analysis indicates a high potential for cracking during construction, the construction procedures could be modified, the material constituents could be changed, or the structural geometry could be redesigned in order to reduce this potential, thereby providing a better product and a more reliable structure. In order to check this potential, an accurate representation of the principal strains are needed coupled with an accurate cracking criterion. ANACAP-U is a subroutine that provides an age-dependent cracking criterion to be used in conjunction with the constitutive model.

Regions of potential cracking are structure, climate, material, and construction-procedure dependent, but several typical situations can be addressed. Structural-related-cracking potential is generally higher at corners and abrupt changes in geometry. Climate-related-cracking potential is generally higher for periods of cold weather during and after construction. Material-related-cracking potential is heavily dependent on the concrete constituents affecting the adiabatic temperature rise, the aging modulus, the creep properties, and/or the shrinkage properties. Constituents that can have a pronounced effect are aggregate size, fly ash content, cement type, and mixtures. Construction-related-cracking potential is heavily dependent on procedures such as placement temperature, insulation, lift height, lift placement rate, lift placement seasons, and/or lift placement sequence.

The potential for cracking at any integration point in a finite element grid is checked using an interactive stress-strain cracking criterion. The cracking criterion is not explicitly time dependent, which is why an interactive stress-strain criterion is used where the time effects are accounted for through the age-dependent modulus. If the cracking criterion is violated, a crack will be introduced perpendicular to the direction of the maximum principal strain. If a crack is introduced, the constitutive matrix is reformulated within the ANACAP-U constitutive subroutine and a new stress state is developed based on zero stress in the principal tensile strain direction. The new constitutive matrix and stresses are then used for subsequent calculations until another crack is indicated by the criterion or until the crack closes. The cracks can close when placed in a compressive state and the material will at that time be capable of carrying compressive loads. Depending on the severity of the crack, the shear resistance is reduced at the cracked integration points, but the crack will have limited shear resistance which is a function of friction and aggregate interlock.

The cracking criterion is both stress and strain dependent. Figure 6, a general plot of experimental fracture data for concrete, shows that fracture can occur in instances of high stress-low strain or high strain-low stress. The triaxial tension and cylinder split tests are of the high stress-low strain variety while the uniaxial compression split test is of the high strain-low stress variety. The latter case is easily explained using a cube loaded in compression on opposite faces, principal stress direction 2 (assuming that principal stresses are arranged from highest tensile to highest compressive). Ultimately, the cube will fracture due to the strain in principal stress direction 1. The stress in this direction will be small tensile stress, which is an indication that fracture is related to the strain. The strain ε_2 would be $-\nu\varepsilon_1$ which would imply that if the compressive stress is approaching the ultimate compressive stress, the cracking strain would be ν times the uniaxial ultimate compressive strain. Since ν is approximately 0.15 to 0.25, the fracture strain would be approximately 15 to 25 percent of the ultimate compressive strain. (A commonly assumed value is 10 percent of the ultimate compressive strain.) Therefore, a strain-dependent cracking criterion seems reasonable. The first case is self-explanatory. Placing a cube in a triaxial state of tension will cause failure prior to reaching the uniaxial tension failure strain; therefore, it is also highly stress dependent.

These two cases indicate that a criterion which is dependent on stress and strain is required. In addition, the time dependency is needed due to aging of the material and creep. Therefore, Figure 6 is approximated by using the fracture strain ε_s (obtained from a slow load test), the fracture stress σ_s (obtained from a slow load test), and the aging modulus $E(\tau)$ to predict the appropriate stress-strain failure surface defined by σ_f and ε_f as shown in Figure 7. The slow load test is performed on a simply supported beam with two point loads applied in a manner to achieve a constant moment in the center of the beam. The load is increased weekly to achieve an increase of tensile stress in the extreme fibers of 25 psi. This procedure is repeated until the beam cracks, providing the slow load fracture strain ε_s, the age of the concrete τ, and the slow load fracture stress σ_s. Previous tests on concrete cylinders using the same mixture as the beam provide the aging modulus $E(\tau)$, which is the last piece of information required to generate the failure surface in Figure 7.

The cracking criterion is either: yes, the material has cracked, or, no, it has not. This yes/no crack prediction is necessary and correct when finding the ultimate response of the structure, but it is not very useful in predicting reliability or potential for cracking. Therefore, the subroutine developed by the ANATECH Research Corp. provides a percentage of the cracking criterion in

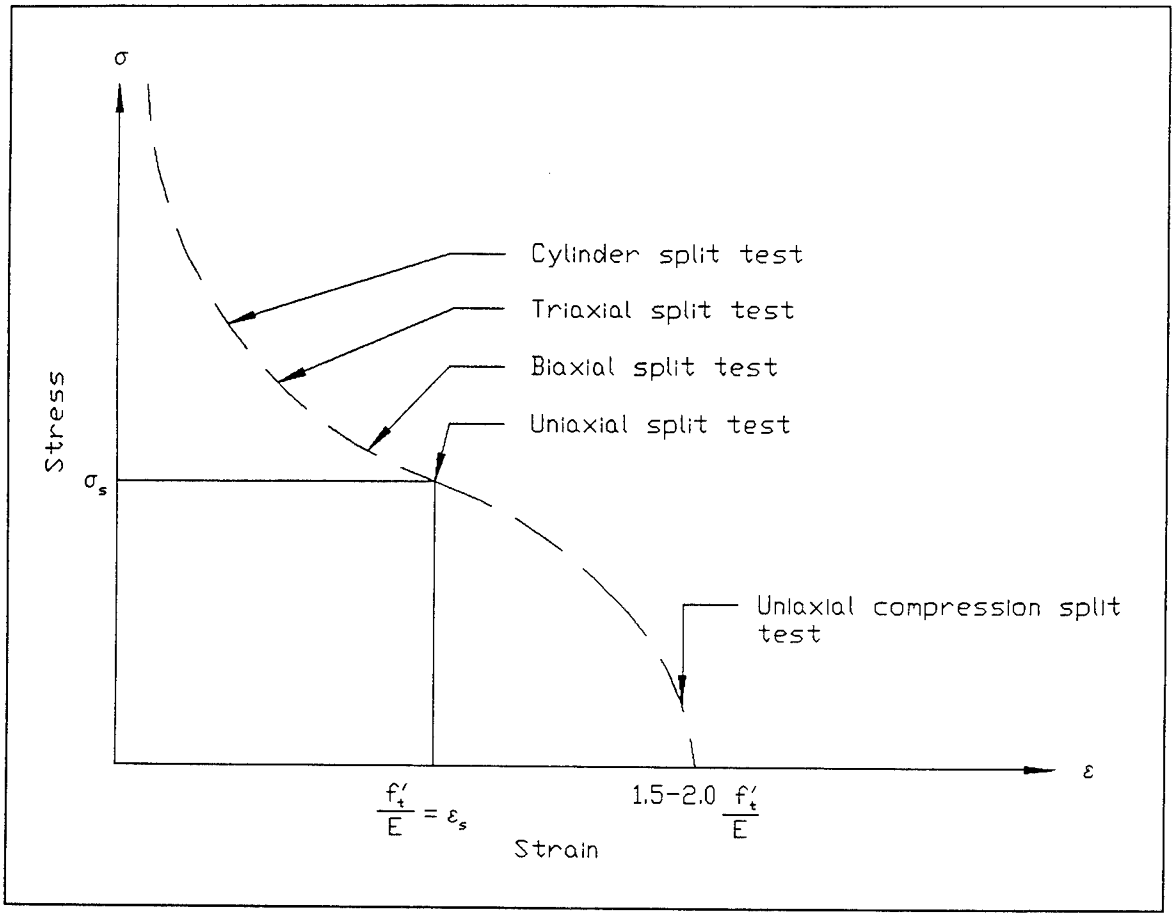

Figure 6. Approximation of stress-strain failure curve based on laboratory test

order to evaluate the potential for cracking. A percentage approaching 100 indicates an increasing possibility of cracking. Any structure with a NISA that indicates a high potential for cracking as described in ETL 1110-2-365 should be evaluated for the severity of the consequences of the predicted cracks. If the consequences are deemed detrimental with respect to either safety or economics, the structure should be redesigned to mitigate the effects or potential of the cracking. Possibilities for redesign include but are not limited to the use of additional reinforcement, the revision of construction procedures, and/or the modification of the material constituents to alleviate or control the cracking.

The cracking criterion is a stress-strain interactive criterion. It accounts for age dependency of the criterion through the use of a linear relationship between cracking stress and cracking strain which is dependent on the aging modulus as shown in Figure 8. With the appropriate values for stress and strain at a given time, Figure 8 can be used to decide if a region of the structure has cracked. If the principal stresses and their respective principal strains, when plotted in Figure 8, are within the triangle enclosed by the failure surface and the two axes, no cracking occurs, and the cracking potential is calculated. If the point of principal stress versus principal strain lies outside the triangle, the concrete has cracked. If the system is assumed to be cracked, the

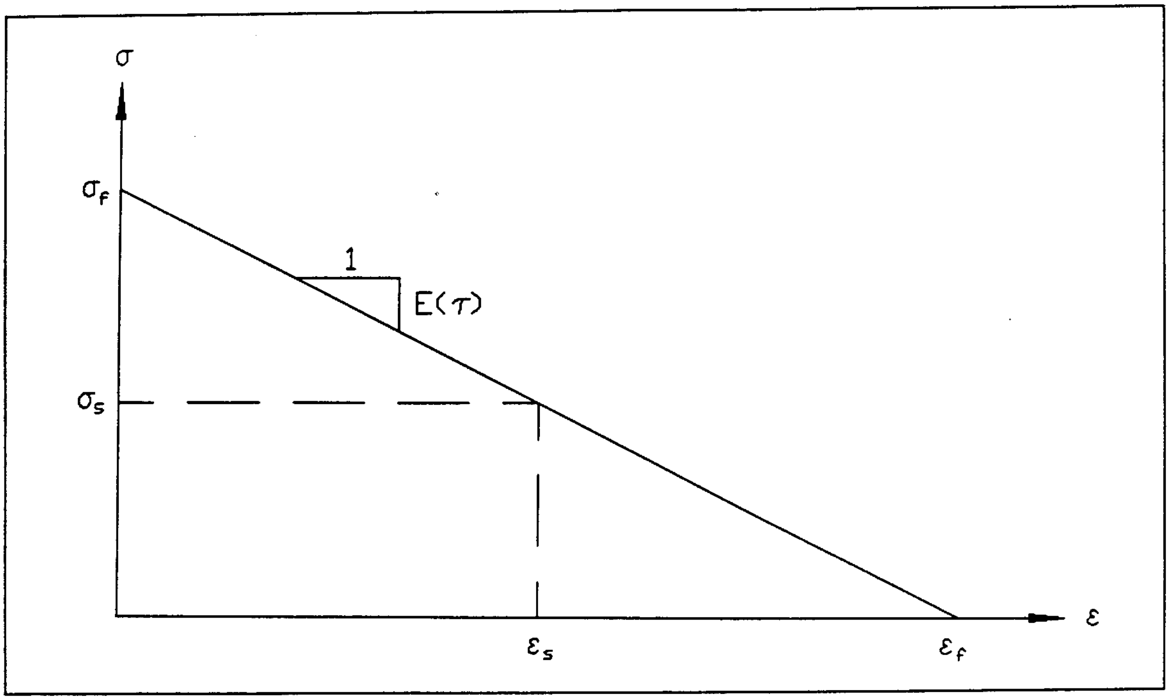

Figure 7. Cracking failure surface and ε_f generation from the slow load fracture test data

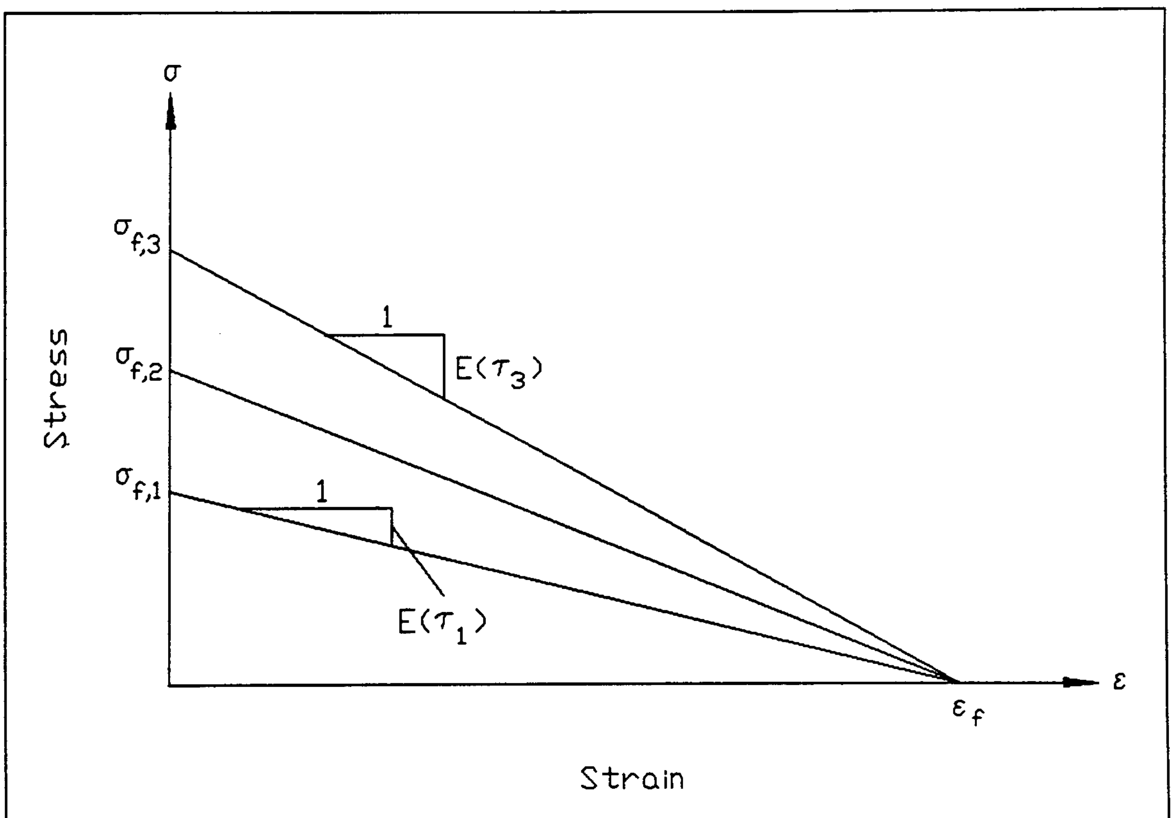

Figure 8. Computer-generated, time-dependent (aging modulus) cracking failure surfaces

constitutive matrix, stress state, nodal forces, and stiffness matrix are adjusted prior to continuation of the analysis.

The failure surface is a function of the fracture stress from the slow load test σ_s, the fracture strain from the slow load test ε_s, and the aging modulus at the time of fracture $E_s(\tau)$, where τ is the age of the concrete. The strain axis intercept is determined as

$$\varepsilon_f = \varepsilon_s + \frac{\sigma_s}{E_s(\tau)} \tag{23}$$

as shown in Figure 7. This intercept value remains constant for the entire NISA and is a prediction of the concrete cracking strain at zero stress. ABAQUS input data require the user to input a cracking strain of

$$\varepsilon_{input} = \frac{1}{2}\varepsilon_f = \frac{1}{2}\left[\varepsilon_s + \frac{\sigma_s}{E_s(\tau)}\right] \tag{24}$$

All of these data are easily obtained from a slow load fracture test. The factor of 1/2 is a function of the input required by the ANATECH-developed subroutine used to generate the correct strain axis intercept used for checking the cracking criterion. Since the strain intercept remains constant, the age dependency is related to the time variation of the aging modulus (Figure 8) for the region of the structure being evaluated for cracking. This concept is illustrated in Figure 8. The stress axis intercept for a given age τ_i is determined as

$$\sigma_{f,i} = \varepsilon_f E(\tau_i) \tag{25}$$

Figure 8 shows three different failure surfaces for the concrete ages of τ_1, τ_2 and τ_3.

Cracking potential is a quantitative measure of the imminence of violating the cracking criteria. It is equivalent to the ratio of l_1 to the total length (l_1 + l_2), as shown in Figure 9, where l_1 is the distance from the origin to the point (ε, σ) which reflects the actual principal stress and strain in the region of the structure being considered for cracking. The value ($l_1 + l_2$) is the length of the line from the origin to the failure surface passing through (ε, σ), which are the strain and stress calculated by the program. The cracking potential is an indicator of how near the current stress-strain state for a given integration point is to the cracking surface.

The following is the algorithm used by the UMAT subroutine to check for cracking as well as the process which occurs when cracking does and does not occur.

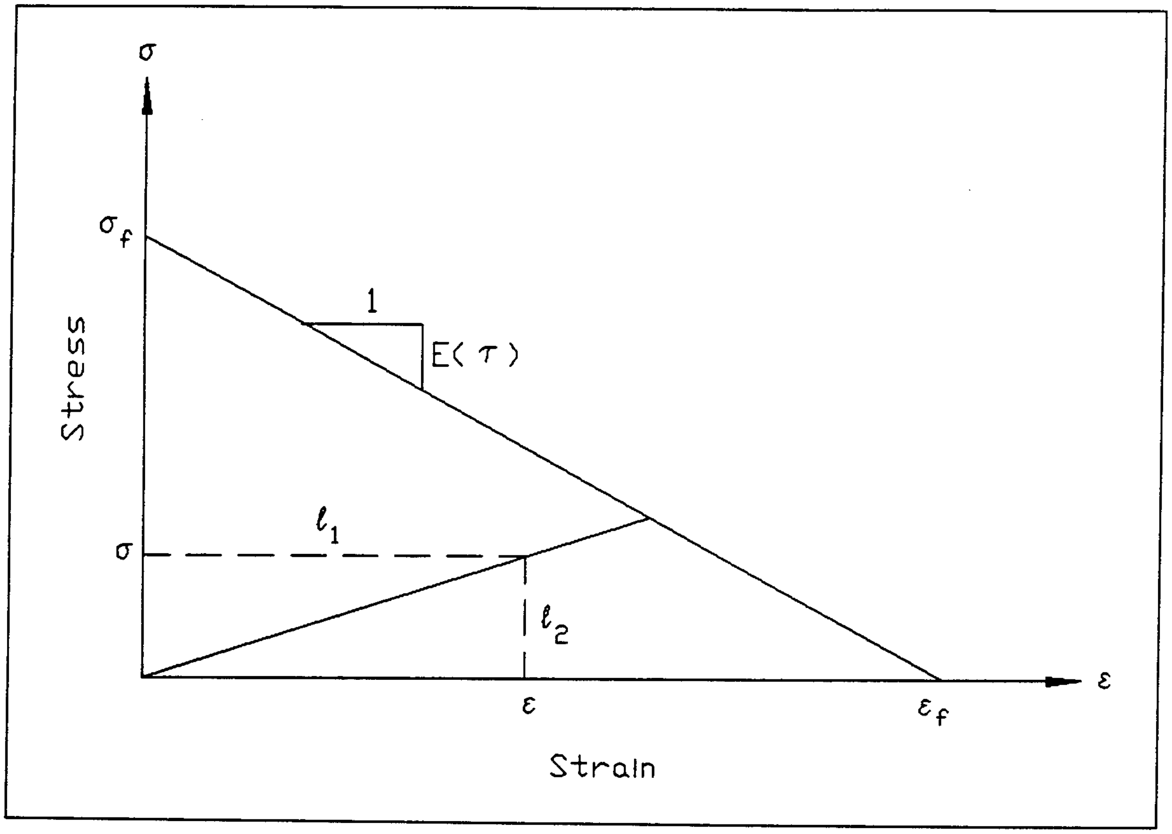

Figure 9. Cracking potential generation for a specific cracking failure surface

a. Plot the point represented by the maximum tensile principal stress σ_1 and its respective principal strain ε_1; check if the point is inside or outside the failure surface.

b. If inside the surface, no cracking occurs, the cracking potential is calculated, and the next integration point is checked.

c. If on or outside the surface, introduce a crack perpendicular to the direction of the maximum tensile principal strain.

d. Then the stress in this direction must be set to zero, and the other stresses must be modified to reflect that change.

e. The stiffness matrix must then be modified to reflect zero load-carrying capabilities in that direction until the crack closes and enters a compressive state.

f. If the material enters a compressive state, the crack is assumed to have closed and 100 percent of the compressive stiffness is reinstated in the direction perpendicular to the crack. Once the material is placed in a tensile state again the crack and a zero stress state is reintroduced at this location.

The 3-D case requires the use of three components of principal stress and strain to determine the cracking potential within the massive concrete structure.

8 Summary

The use of an accurate constitutive model is imperative when performing a mass concrete NISA. ANATECH Research Corporation's ANACAP-U, constitutive relationship, software coupled with the general-purpose finite element program ABAQUS provide the means for performing reliable NISAs. The ANACAP-U constitutive model equations can be adapted to fit the experimental data for a given project, and this experimentally based constitutive model can then be implemented with ABAQUS' user-defined material property subroutines to accurately analyze the mass concrete structure. The creep, shrinkage, aging modulus, and cracking criteria are modeled within ANACAP-U and are considered the minimum necessary properties for accurate modeling of the material behavior. The general theories used within the constitutive model have been presented within this report in a practical manner to enhance the user's knowledge regarding the use of material constitutive law modeling and its use in analyzing structural behavior. This practical discussion is far from being all-inclusive and users of the ANACAP-U constitutive model should read its manual carefully and only deviate from that manual after obtaining a thorough understanding of the software and material modeling concepts. The use of these constitutive models and the development of the appropriate constants within the equations representing the material properties should be a joint or team effort including the materials, structural, and construction engineering staff for the project. The intent of performing a NISA is to provide more reliable and cost-effective structures and the use of an accurate constitutive or material model is necessary for this intent to become a reality.

References

ANATECH Research Corp. (1992). *ANACAP-U ANATECH concrete analysis package, version 92-2.2 user's manual.* San Diego, CA.

Fehl, B. D., Riveros, G. A., and Garner, S. A. (in preparation). "Nonlinear, incremental structural analysis of McAlpine locks replacement project," Technical Report ITL-95- , U.S. Army Engineer Waterways Experiment Station, Vicksburg, MS.

Fintel, M., ed. (1974). "Handbook of concrete engineering," Van Nostrand Reinhold Co., New York, NY.

U.S. Army Corps of Engineers (USACE). (1994). Engineer Technical Letter 1110-2-365, "Nonlinear incremental structural analysis of massive concrete structures," Washington, DC.

U.S. Army Engineer District, Louisville (USAED, Louisville). (1993). "Concrete materials, McAlpine Lock replacement, Ohio River," Design Memorandum No. 1, Louisville, KY.

Appendix A Calibration of Creep Curve to Data—Example

Calibration of the creep curve is somewhat more involved than calibration of the modulus of elasticity and the shrinkage curves since the equations in the constitutive model for creep are not directly correlated to the test data. The modulus and the shrinkage can be computed with the equations and compared directly with the test results. For creep, once an equation has been defined, a numerical simulation of the test must be performed. The numerically generated results are then compared with the plots of the test results. As described in the main body of this report, steps can be taken to obtain a first approximation of the equation of the creep curve, but this will rarely provide the final parameters needed to satisfy a reasonable calibration process.

In order to obtain an accurate equation for creep, an iterative process is usually required which involves changing a parameter in the equation, performing the numerical analysis of the test, and comparing the results with the test data. After viewing the results, this process may need to be performed again. There is no specific number of iterations required and they will vary from one concrete mixture to the next. This appendix was assembled to demonstrate the process that is required to obtain a fit of the creep curve equation to the test data.

The test data used in the calibration process presented in this appendix are for the interior mixture from the McAlpine Lock Replacement project. A full set of tests was conducted for the McAlpine project as part of the material characterization study (1994, DM No. 1, Concrete Materials, McAlpine Lock Replacement)[1] and for the nonlinear, incremental structural analysis (NISA) that was performed (in preparation, Fehl, Riveros, and Garner).

Using the process to define the creep equation as outlined in the main body of the report, 3-day creep data were selected as the basis for establishing the parameters. The times selected for curve fitting were 4, 20, and 100 days.

[1] References cited in this appendix are located at the end of the main text.

Using these times and assuming the exponential terms of Equation 4 of the main text are equal to a value of 0.001, values for r_1, r_2, and r_3 can be computed as follows:

$$e^{-r_1(4-3)} = 0.001 \quad \Rightarrow r_1 = 6.9078$$

$$e^{-r_2(20-3)} = 0.001 \quad \Rightarrow r_2 = 0.4063$$

$$e^{-r_3(100-3)} = 0.001 \quad \Rightarrow r_3 = 0.0721$$

For this case the constant term in Equation 4 was replaced with a third exponential.

Now that values for r_1, r_2, and r_3 have been computed they can be substituted into the equation. The values for $J(t,\tau)$ for times t of 4, 20, and 100 days and τ of 3 days can be found from the test data in the material characterization study report (USAED Louisville 1993) and substituted into the equation. Values from the McAlpine project study were:

$$J(4,3) = 0.2 \text{ millionths/psi}$$

$$J(20,3) = 0.6 \text{ millionths/psi}$$

$$J(100,3) = 0.8 \text{ millionths/psi}$$

So, once the values for r_1, r_2, and r_3 and $J(t,\tau)$ are substituted, then three equations with three unknowns remain and can be solved simultaneously. The three equations are:

$$0.2 \times 10^{-6} = 0.999A_1 + 0.3339A_2 + 0.0687A_3 \tag{A1}$$

$$0.6 \times 10^{-6} = A_1 + 0.999A_2 + 0.2980A_3 \tag{A2}$$

$$0.8 \times 10^{-6} = A_1 + A_2 + 0.999A_3 \tag{A3}$$

Solving the equations simultaneously results in the following values for A_1, A_2, and A_3:

$$A_1 = 0.12513 \times 10^{-6}$$

$$A_2 = 0.3904 \times 10^{-6}$$

$$A_3 = 0.28475 \times 10^{-6}$$

These values along with those computed above for r_1, r_2, and r_3 can be used in the equation for creep in the constitutive model and a numerical analysis of the creep cylinder tests can be performed. The strains from these analyses can be be compared with the actual strains recorded during the test to determine if the parameters computed are adequate.

The analyses were performed using these initial parameters and the results from the analyses are compared with the test results in Figure A1 for the 1-day, 3-day, and 14-day creep tests. The magnitudes are approximately correct for the 3- and 14-day tests but the shape of the curves is not satisfactory for these two tests. Adjustments must be made and then the analyses performed again and the results compared with the test results.

Magnitudes of the curves are generally controlled by the factors while the shapes of the curves can be changed by adjusting the exponentials. Since the results from the analysis are decreasing compared with the test results, the exponential for the long term (r_3) will be adjusted as shown in Table A1 for attempt No. 2. Results of the analysis using values for attempt No. 2 and results from attempt No. 1 and from the test data are shown in Figure A2. The long-term shapes are improved but the results are too low for the 3- and 14-day tests.

Since the early time drop appears to be excessive, the exponent for early times will be reduced to change the behavior of the early time curve. Attempt No. 3 will revise exponent r_1 as shown in Table A1. The results of attempt No. 3 are shown in Figure A3 and are compared with the results from attempt No. 2 and the test data. The revised exponent changed the early time behavior of the curve slightly and increased the strain recorded for all three tests, but the values are still low and the increase in strain is still too gradual.

To increase the steepness of the curve in the first 50 days, the exponential term r_1 will be reduced further as shown in Table A1. Exponent r_3 will also be changed to flatten the long-term curve. The results of attempt No. 4 are shown in Figure A4 and are compared with the results of attempt No. 3 and the test data. In all three tests the curve is now approaching a shape comparable to that of the test data, but the magnitude of the strains is too low for the 3- and 14-day tests.

To increase the magnitude of the strains, the A_2 term will be increased to revise the overall magnitude of the curve. The change made for attempt No. 5 can be seen in Table A1, and the results of the analyses are shown in Figure A5 and are compared with results from attempt No. 4 and the test data. As can be seen in Figure A5 the numerical results now exceed the values from the test data for all three tests.

Two parameters will be changed on the next attempt. The early time factor A_1 will be increased substantially to maintain the steep curve at early times and factor A_3 will also be decreased significantly to try and maintain a flat curve at later times. The changes made are shown in Table A1 and the results shown in Figure A6. As can be seen in Figure A6 the change in parameters basically decreased the steepness of the slope and the magnitudes are still too high at longer times.

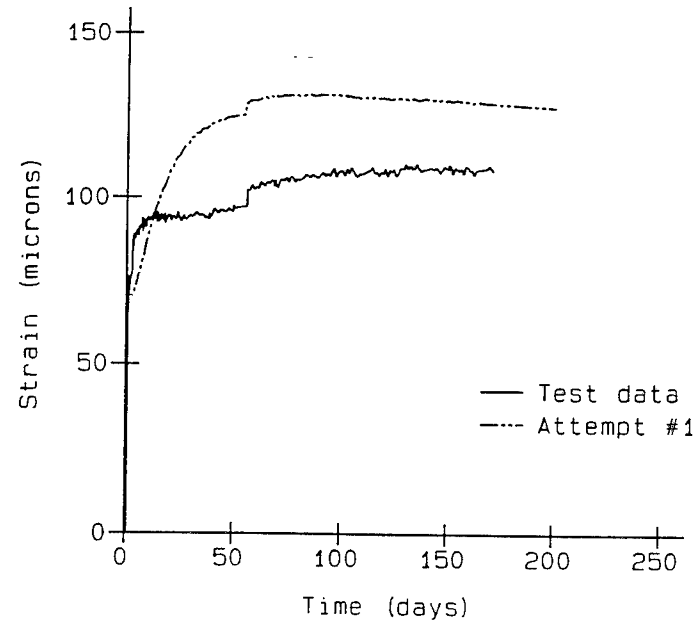

a. 1-day test

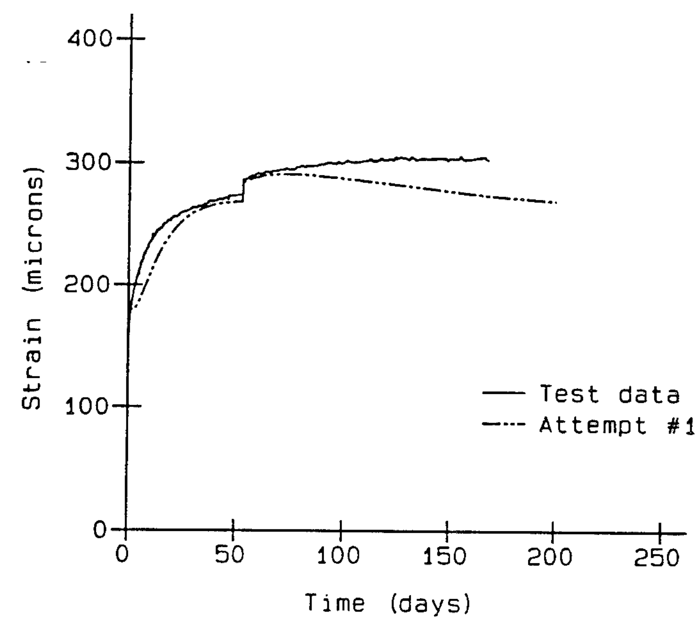

b. 3-day test

Figure A1. Time history strain plots of creep test data and numerical results for attempt No. 1 (Continued)

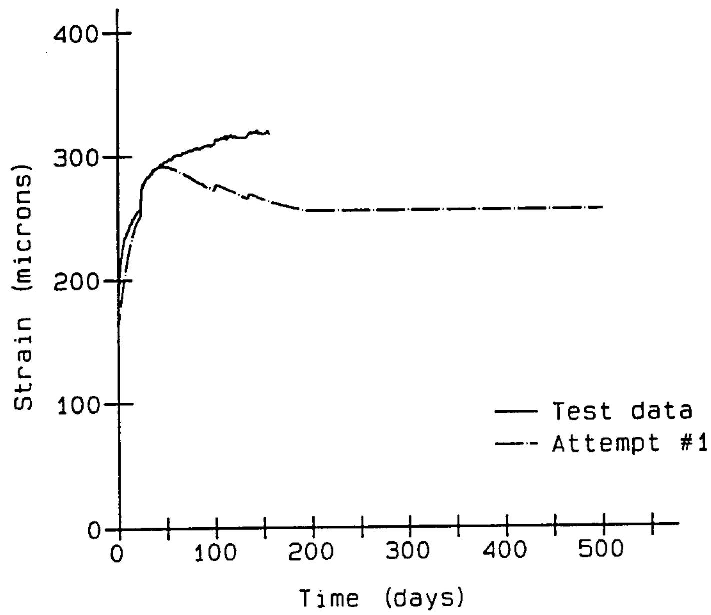

c. 14-day test

Figure A1. (Concluded)

Table A1
Exponentials and Factors Used in Calibrating Creep Curve

Attempt No.	Exponentials			Factors		
	r_1	r_2	r_3	A_1	A_2	A_3
1	6.9078	0.4063	0.07121	0.1674	-0.0402	0.6735
2	6.9078	0.4063	0.02	0.1674	-0.0402	0.6735
3	1.0	0.4063	0.02	0.1674	-0.0402	0.6735
4	0.1	0.4063	0.03	0.1674	-0.0402	0.6735
5	0.1	0.4063	0.03	0.1674	0.2	0.6735
6	0.1	0.4063	0.03	0.7	0.2	0.1
7	1.0	0.2	0.01	0.7	0.2	0.1
8	1.0	0.2	0.01	0.15	0.2	0.5
9	1.0	0.2	0.01	0.15	0.4	0.5
10	1.0	0.2	0.02	0.15	0.4	0.3

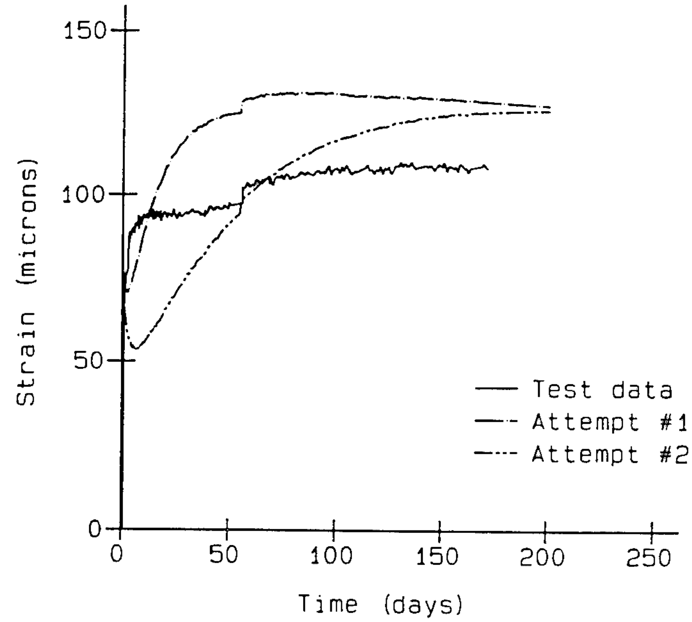

a. 1-day test

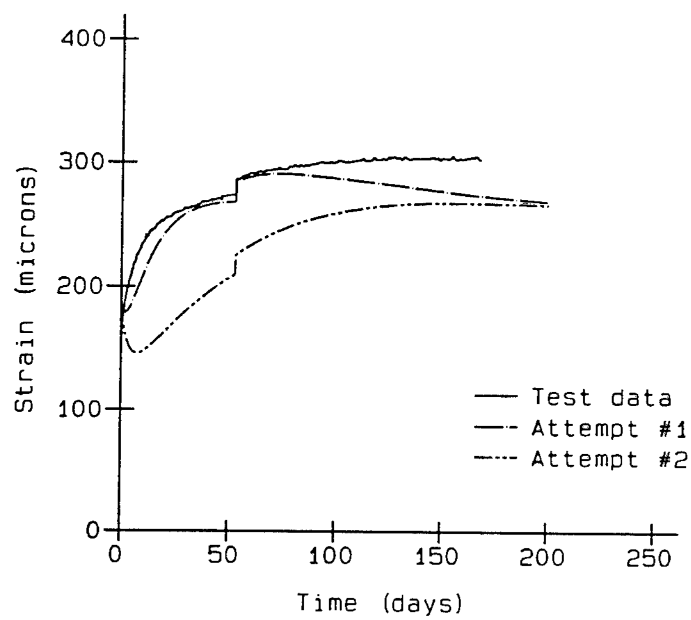

b. 3-day test

Figure A2. Time history strain plots of creep test data and numerical results for attempts No. 1 and 2 (Continued)

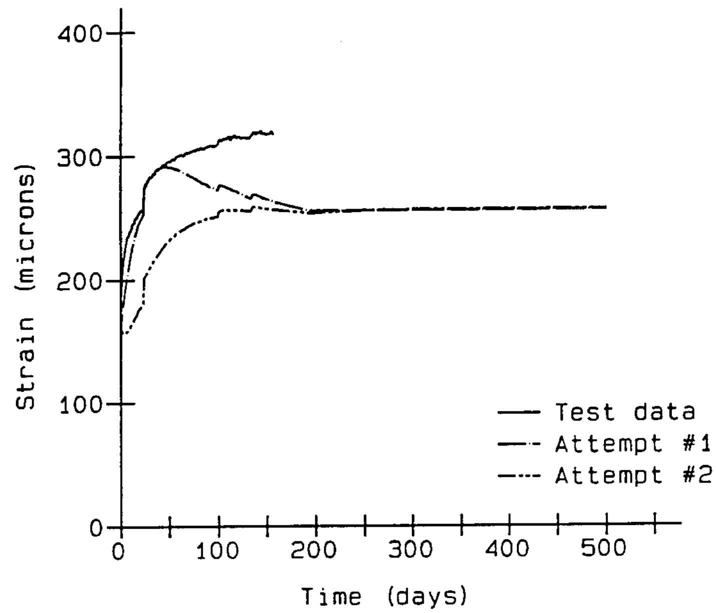

c. 14-day test

Figure A2. (Concluded)

Since steepness of the curves again appears to be a problem, the exponential terms will again be adjusted. This time all three exponentials will change as shown in Table A1 with resulting plots as shown in Figure A7. The changes made increased the early-time steepness of all three curves significantly but did result in a reduction in magnitude of strains at later times.

Since an earlier increase in A_1 (attempt No. 6) caused a significant increase in the steepness of the early-time curve, A_1 will now be reduced to near its original value as shown in Table A1. To account for the loss in magnitude, factor A_3 will be increased. Figure A8 shows the results and as can be seen the curve is now much flatter but the magnitude is too low except for the 1-day test. In addition, curves for 3 and 14 days should be a little steeper at early times.

To get the order of magnitude correct for the 3- and 14-day curves, the factor A_2 will be increased as shown in Table A1. The effect of this increased factor is shown in Figure A9 where curves for 3 and 14 days are getting very close to the test values. Magnitudes are still a little high on the 3-day curve and the steepness of the curve over the long term should be decreased slightly. Values for the 1-day creep are too high, but it is becoming apparent that exponents and factors that can be used to fit the 3- and 14-day curves will not provide good agreement with the 1-day curve.

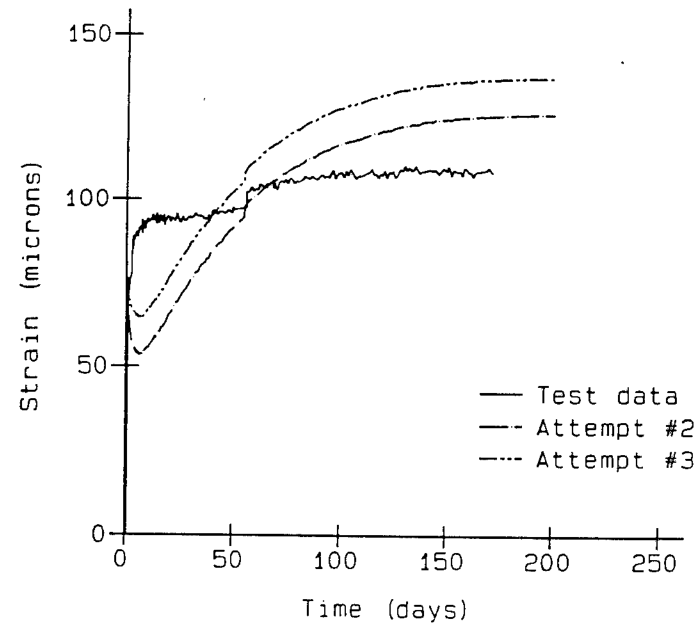

a. 1-day test

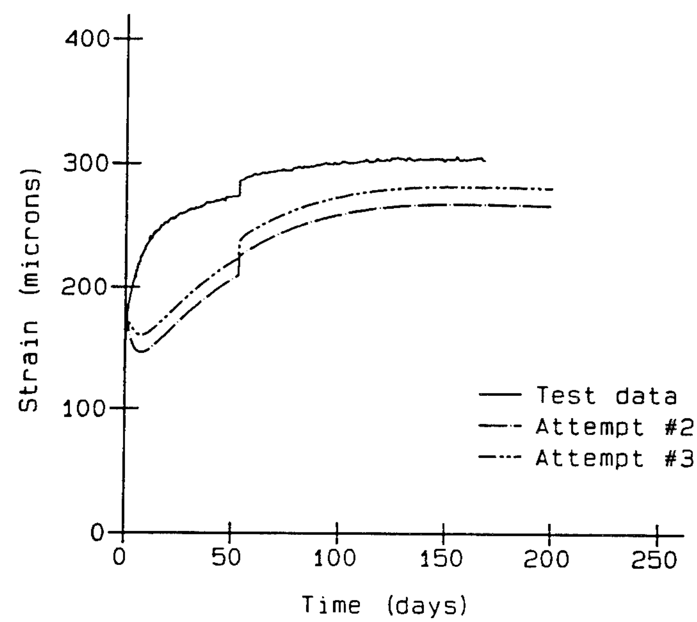

b. 3-day test

Figure A3. Time history strain plots of creep test data and numerical results for attempts No. 2 and 3 (Continued)

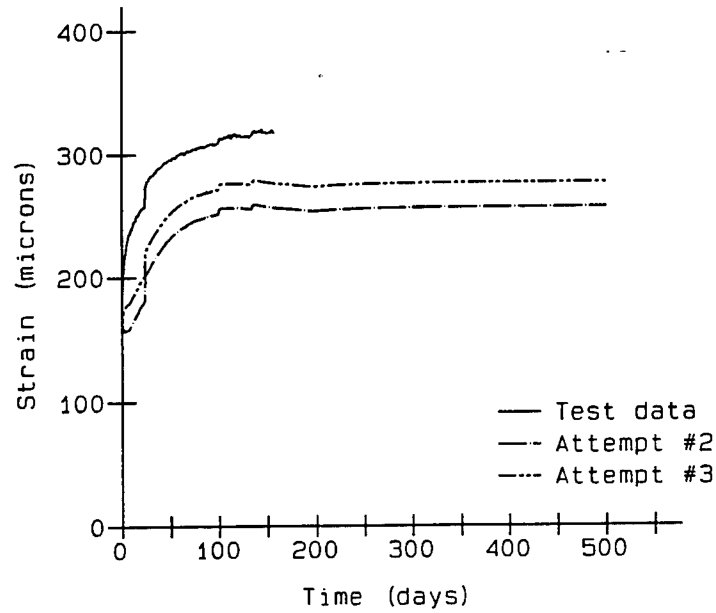

c. 14-day test

Figure A3. (Concluded)

The tenth attempt will increase the exponent r_2 to flatten the curve somewhat and the factor A_3 will be decreased to reduce the magnitude over the long term. The changes are shown in Table A1 and the results are plotted in Figure A10. As can be seen in Figure A10 the magnitude of strains decreased for all three tests for the portion of the curves beyond 50 days. Figure A10(b) shows that the data for attempt No. 10 provide very good agreement for the 3-day data and reasonable agreement with the 14-day data as shown in Figure A10(c). As stated in the paragraph above, a discrepancy exists for the 1-day creep test results but this does not appear to be able to be resolved without ruining the fits of the 3- and 14-day curves.

The curve fits shown for attempt No. 10 in Figure A10 could be adjusted further to try to account for the high values for the 1-day test and to increase values at the later times for the 14-day test. A decision could also be made to select attempt No. 9 factors and exponentials since these values provide an excellent fit with the 14-day creep data. The difficulty always with calibrating the creep curve though is that a change made to correct a deficiency in the fit for one curve will affect the other two curves. Although difficult, factors and exponentials can be found that will accurately reflect all three sets of the test, but generally fitting the data to two of the curves will have to suffice.

As can be seen by the steps taken in this appendix to calibrate a creep curve, the process can be tedious. The process was presented to provide the

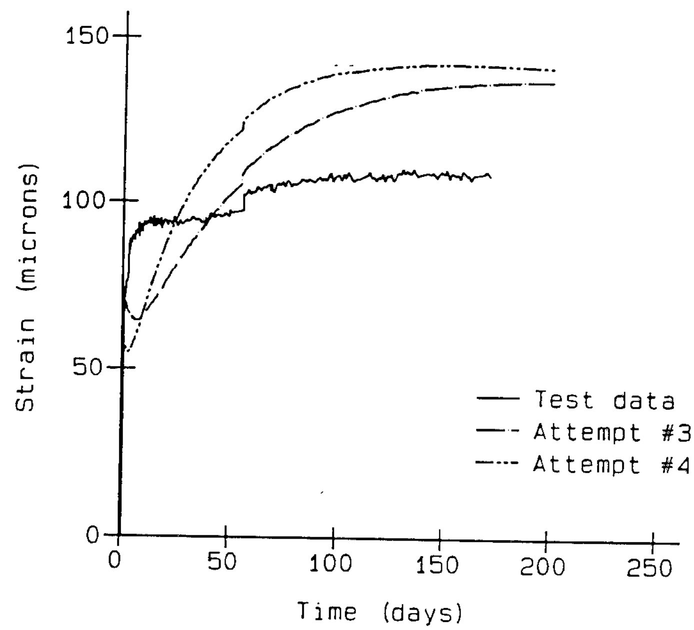

a. 1-day test

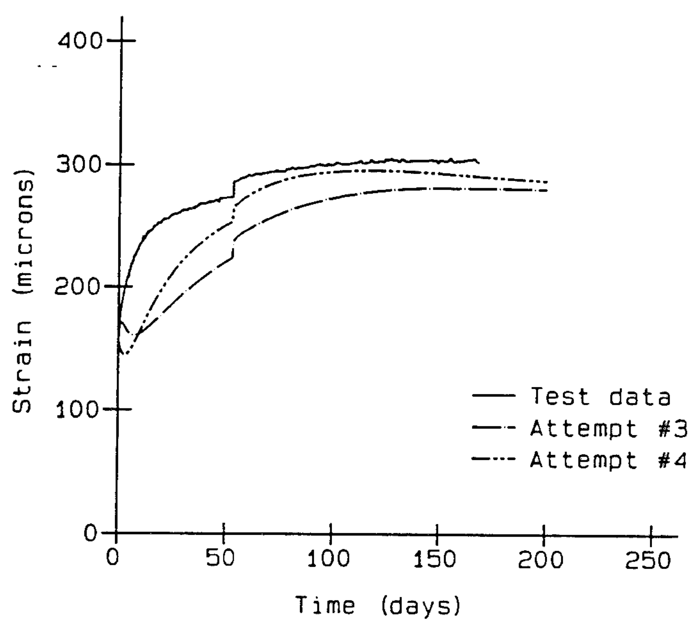

b. 3-day test

Figure A4. Time history strain plots of creep test data and numerical results for attempts No. 3 and 4 (Continued)

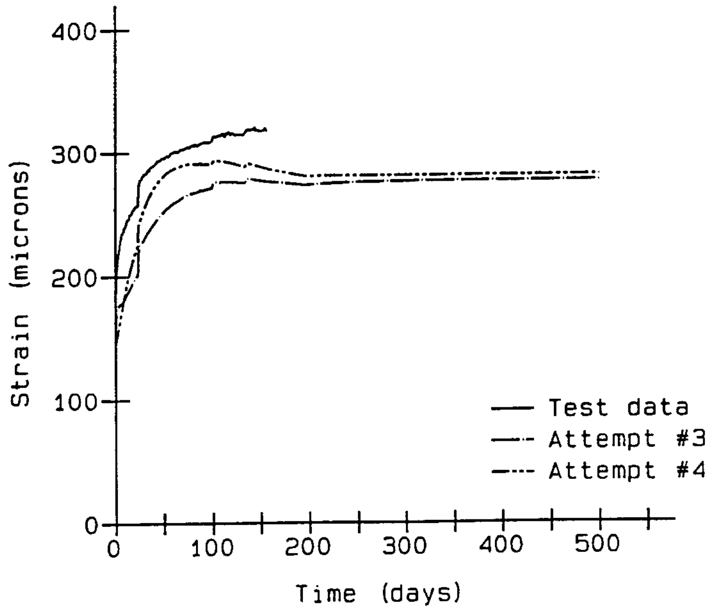

c. 14-day test

Figure A4. (Concluded)

reader a better understanding of how involved the process of calibrating the creep equation can be and to provide insight on how to adjust the parameters. Calibration of the creep curve is certainly not exact but through careful manipulation of the parameters and use of good engineering judgment a set of parameters can be found which adequately capture the creep behavior.

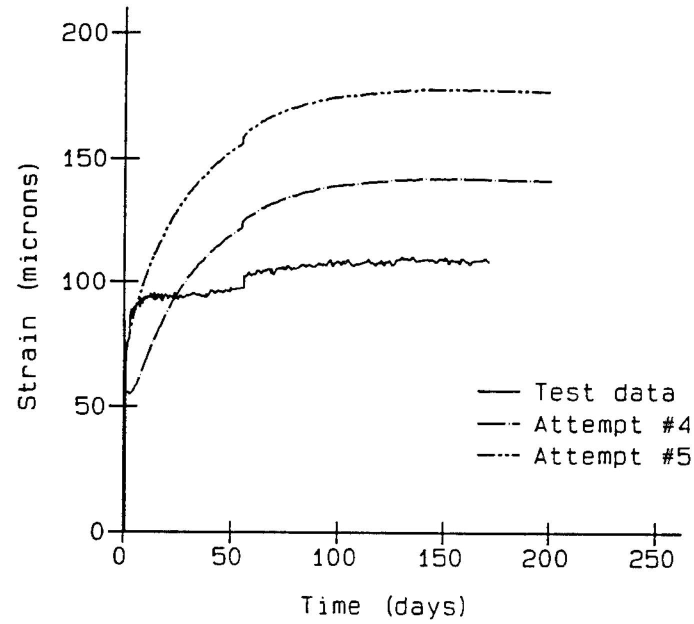

a. 1-day test

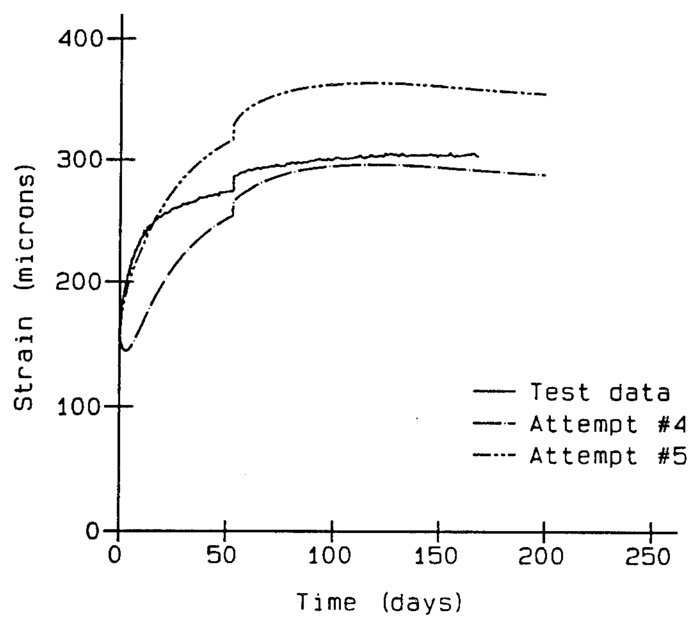

b. 3-day test

Figure A5. Time history strain plots of creep test data and numerical results for attempts No. 4 and 5 (Continued)

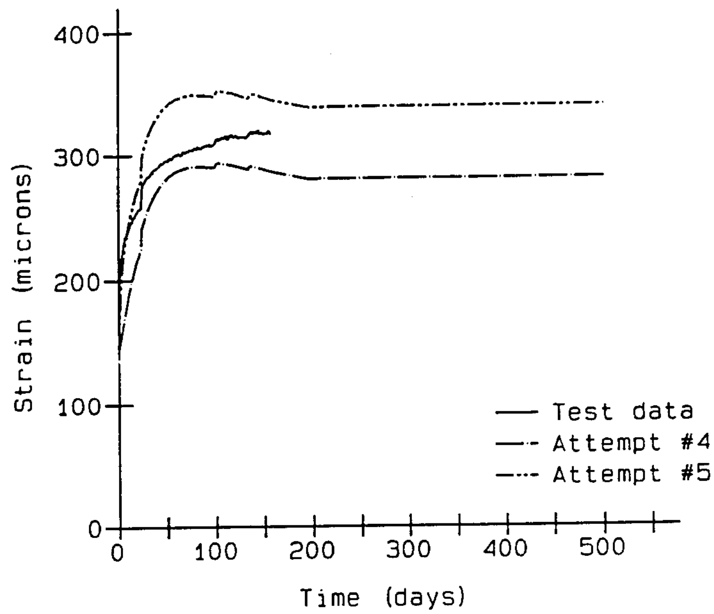

c. 14-day test

Figure A5. (Concluded)

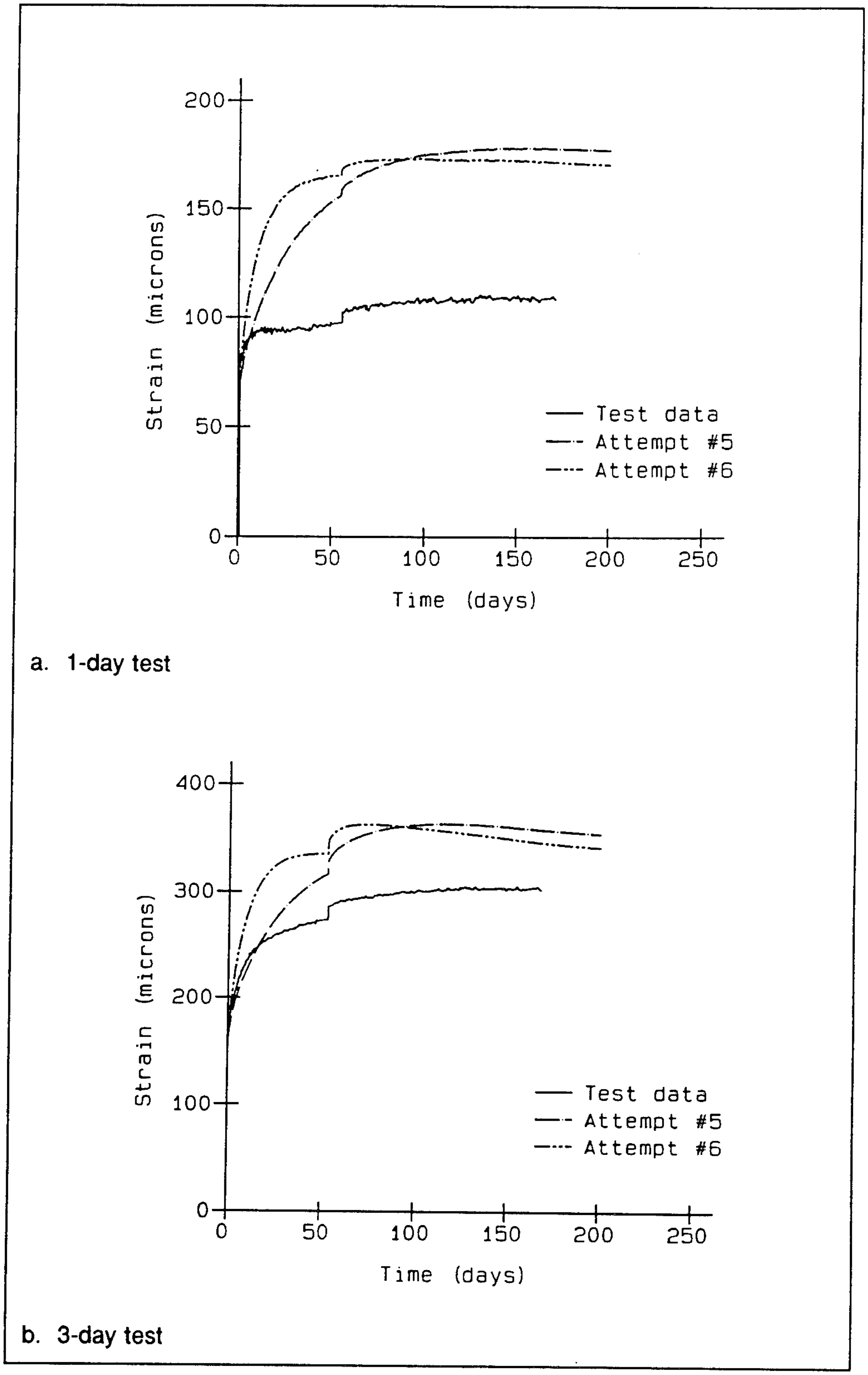

Figure A6. Time history strain plots of creep test data and numerical results for attempts No. 5 and 6 (Continued)

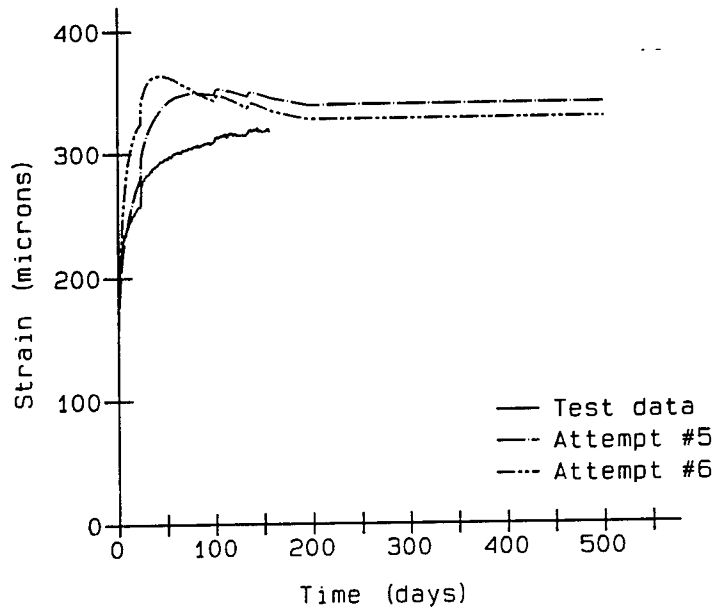

c. 14-day test

Figure A6. (Concluded)

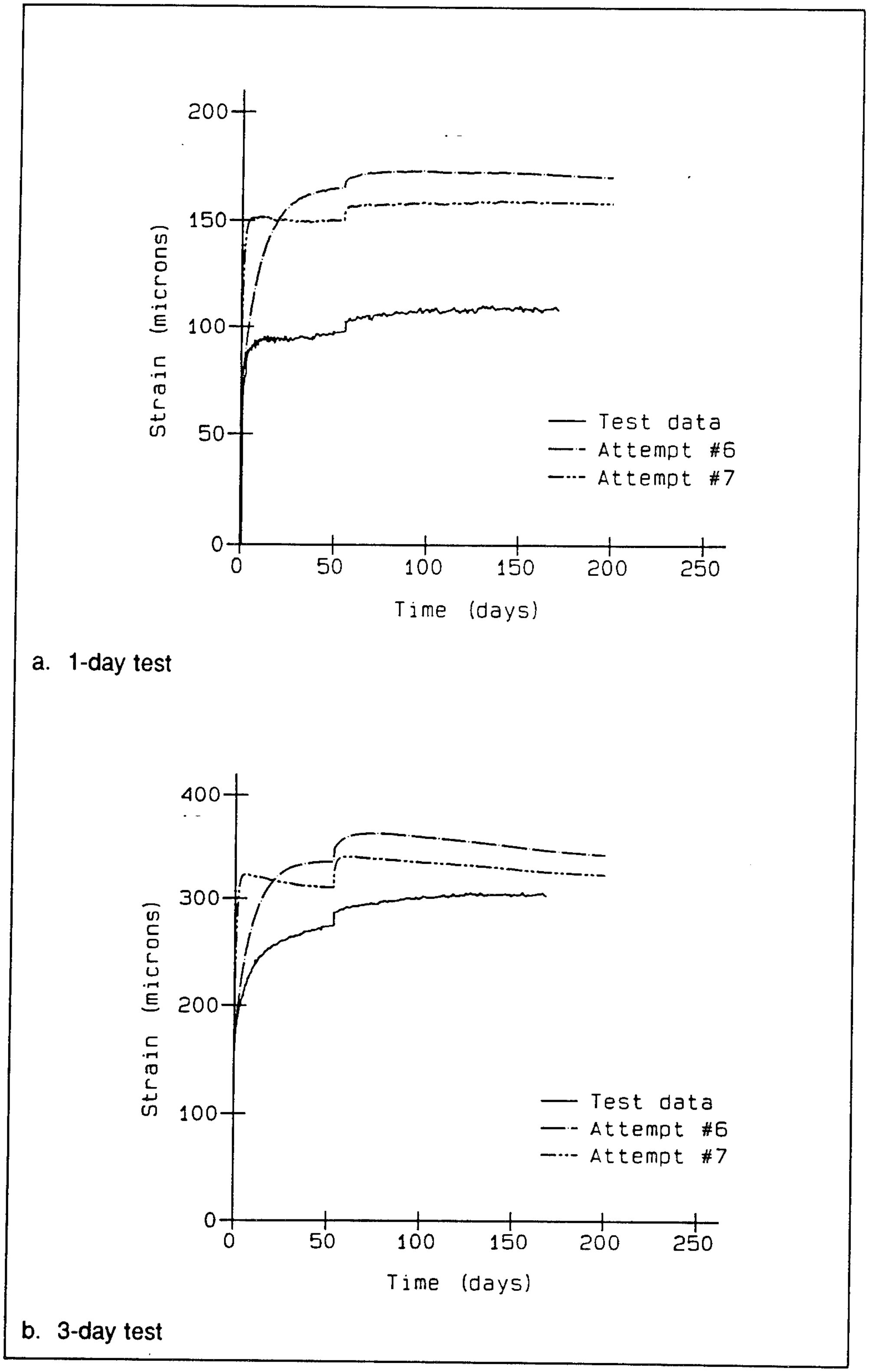

Figure A7. Time history strain plots of creep test data and numerical results for attempts No. 6 and 7 (Continued)

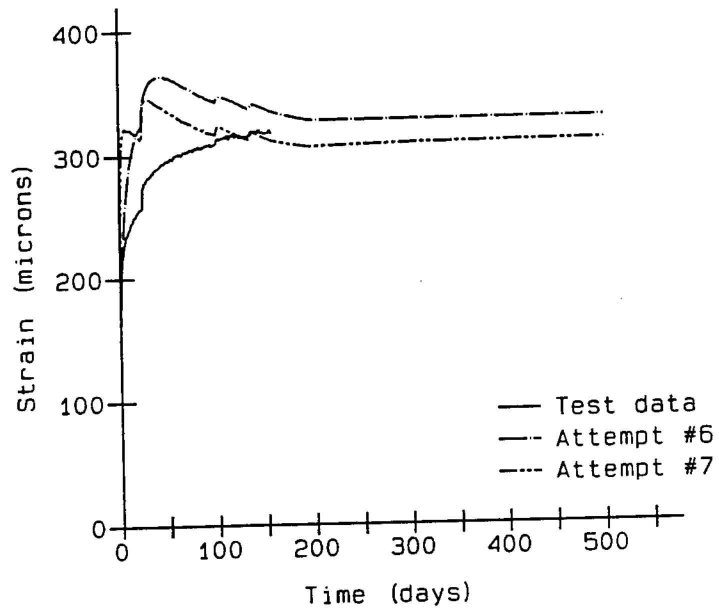

c. 14-day test

Figure A7. (Concluded)

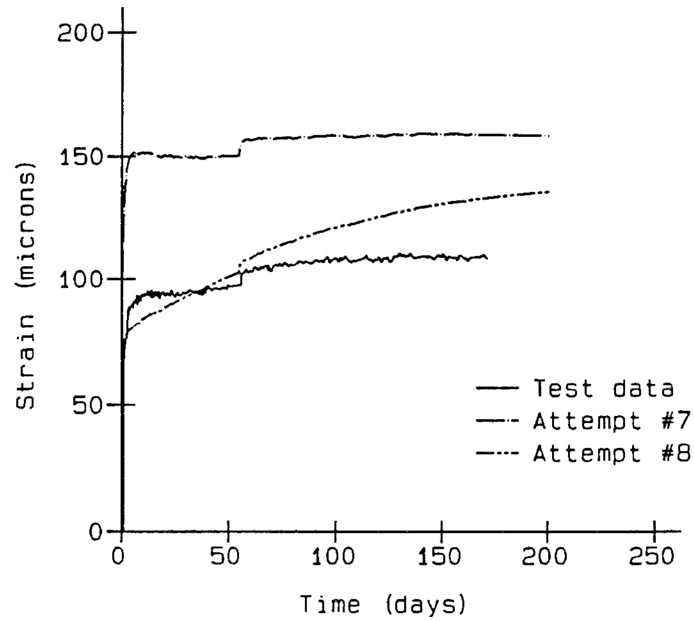

a. 1-day test

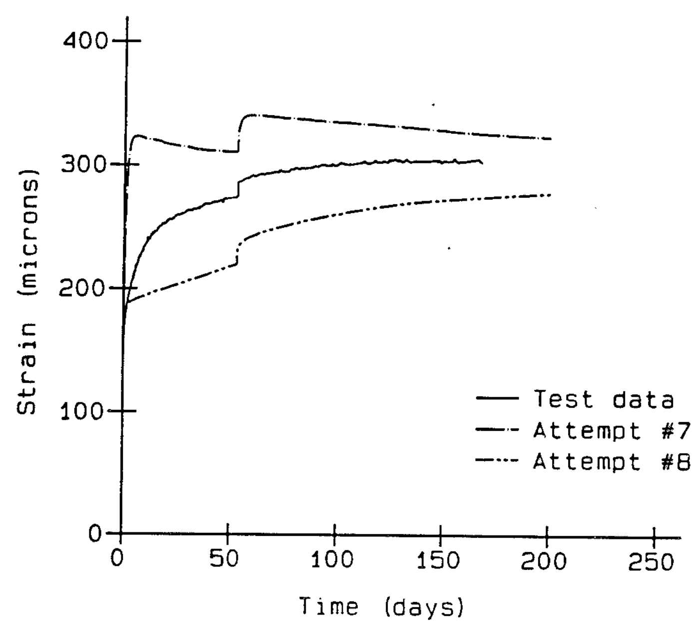

b. 3-day test

Figure A8. Time history strain plots of creep test data and numerical results for attempts No. 7 and 8 (Continued)

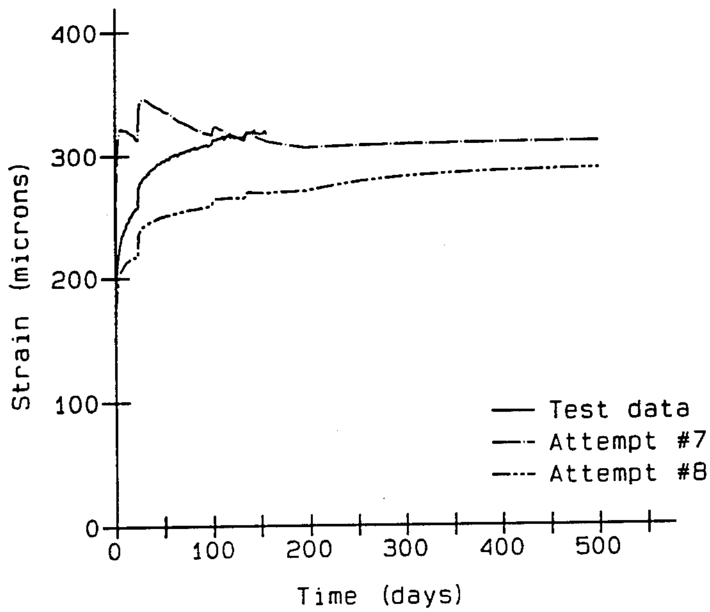

c. 14-day test

Figure A8. (Concluded)

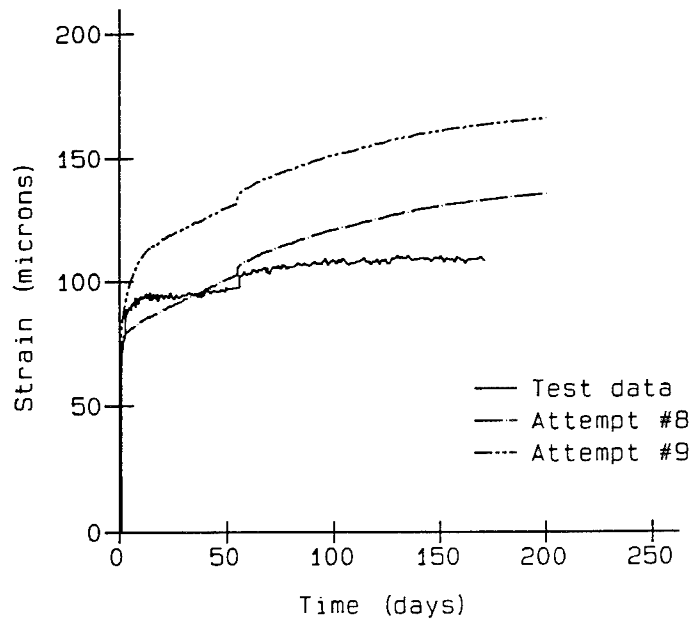

a. 1-day test

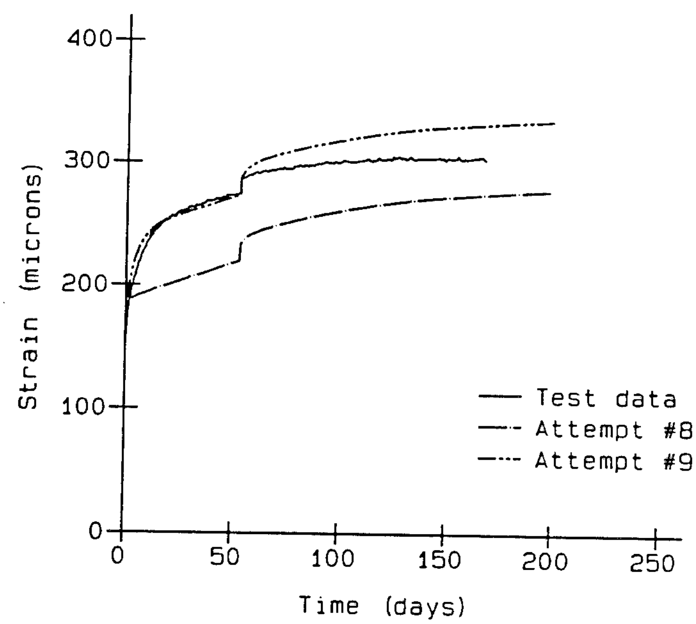

b. 3-day test

Figure A9. Time history strain plots of creep test data and numerical results for attempts No. 8 and 9 (Continued)

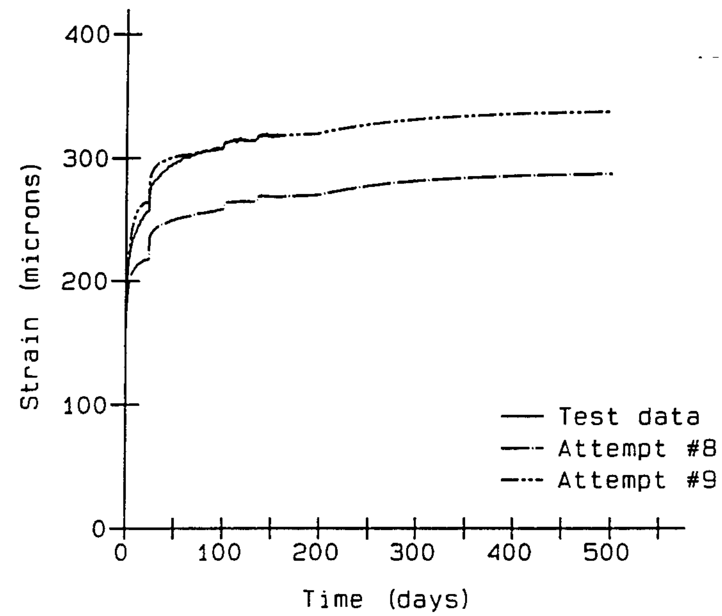

c. 14-day test

Figure A9. (Concluded)

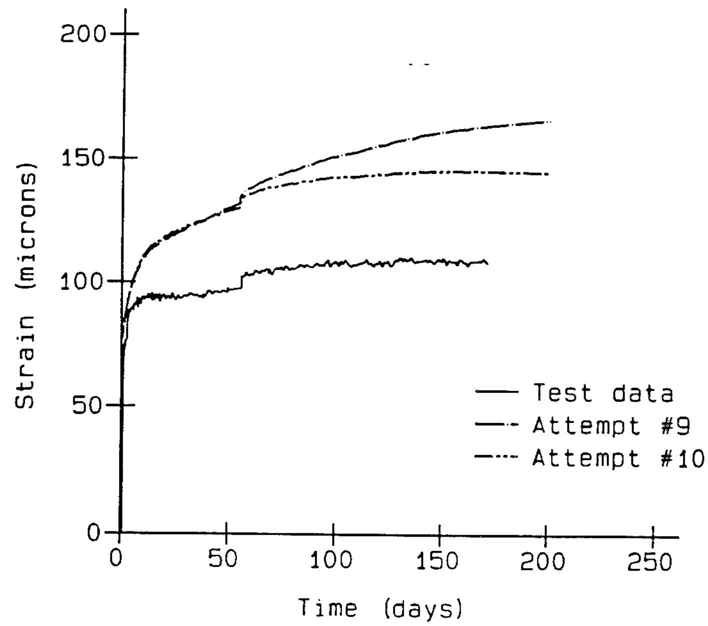

a. 1-day test

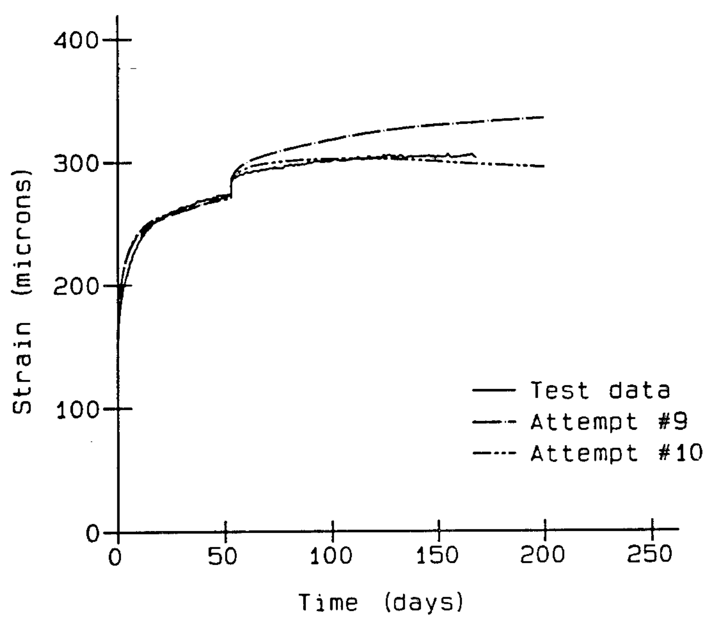

b. 3-day test

Figure A10. Time history strain plots of creep test data and numerical results for attempts No. 9 and 10 (Continued)

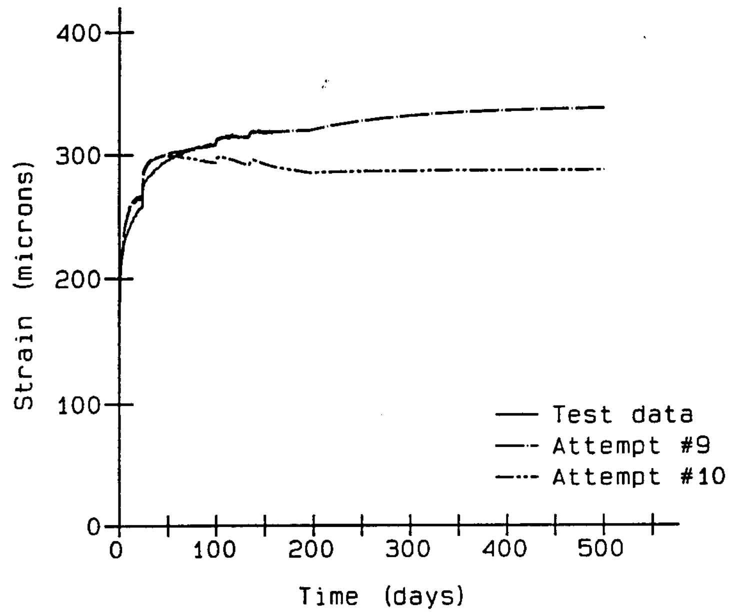

c. 14-day test

Figure A10. (Concluded)

REPORT DOCUMENTATION PAGE

Form Approved
OMB No. 0704-0188

1. AGENCY USE ONLY *(Leave blank)*

2. REPORT DATE
September 1995

3. REPORT TYPE AND DATES COVERED
Final report

4. TITLE AND SUBTITLE
Constitutive Modeling of Concrete for Massive Concrete Structures, A Simplified Approach

5. FUNDING NUMBERS

6. AUTHOR(S)
Kevin Z. Truman, Barry D. Fehl

7. PERFORMING ORGANIZATION NAME(S) AND ADDRESS(ES)
Washington University, Dept. of Civil Engineering, One Brookings Drive, St. Louis, MO 63130; U.S. Army Engineer Waterways Experiment Station, Information Technology Laboratory, 3909 Halls Ferry Road, Vicksburg, MS 39180-6199

8. PERFORMING ORGANIZATION REPORT NUMBER
Technical Report ITL-95-8

9. SPONSORING/MONITORING AGENCY NAME(S) AND ADDRESS(ES)
Headquarters, U.S. Army Corps of Engineers
Washington, DC 20314-1000

10. SPONSORING/MONITORING AGENCY REPORT NUMBER

11. SUPPLEMENTARY NOTES
Available from National Technical Information Service, 5285 Port Royal Road, Springfield, VA 22161.

12a. DISTRIBUTION/AVAILABILITY STATEMENT
Approved for public release; distribution is unlimited.

12b. DISTRIBUTION CODE

13. ABSTRACT *(Maximum 200 words)*

Basic concepts and ideas pertaining to a constitutive model that is used in nonlinear, incremental structural analysis (NISA) of massive concrete structures are presented. The information is presented in such a manner that the practicing engineer can read the report and understand how it is used. (Rigorous derivations of the equations used in the constitutive model are not included for the sake of clarity.)

The constitutive model contains time-dependent properties for the modulus of elasticity, creep, and shrinkage that can be calibrated against test results. A smeared crack model is also contained in the constitutive model and provides a prediction of concrete cracking based on both the stress and strain. The theory behind the equations used to model the material properties as well as the cracking criteria are presented.

Also included is information regarding the input needed for a given material (or materials) and steps that must be taken to calibrate the constitutive model for a specific concrete mixture.

14. SUBJECT TERMS
Concrete
Constitutive model
Cracking
Nonlinear properties

15. NUMBER OF PAGES
65

16. PRICE CODE

17. SECURITY CLASSIFICATION OF REPORT
UNCLASSIFIED

18. SECURITY CLASSIFICATION OF THIS PAGE
UNCLASSIFIED

19. SECURITY CLASSIFICATION OF ABSTRACT

20. LIMITATION OF ABSTRACT

NSN 7540-01-280-5500

Standard Form 298 (Rev. 2-89)
Prescribed by ANSI Std. Z39-18
298-102

WATERWAYS EXPERIMENT STATION REPORTS PUBLISHED UNDER THE COMPUTER-AIDED STRUCTURAL ENGINEERING (CASE) PROJECT

	Title	Date
Technical Report K-78-1	List of Computer Programs for Computer-Aided Structural Engineering	Feb 1978
Instruction Report O-79-2	User's Guide:Computer Program with Interactive Graphics for Analysis of Plane Frame Structures (CFRAME)	Mar 1979
Technical Report K-80-1	Survey of Bridge-Oriented Design Software	Jan 1980
Technical Report K-80-2	Evaluation of Computer Programs for the Design/Analysis of Highway and Railway Bridges	Jan 1980
Instruction Report K-80-1	User's Guide:Computer Program for Design/Review of Curvilinear Conduits/Culverts (CURCON)	Feb 1980
Instruction Report K-80-3	A Three-Dimensional Finite Element Data Edit Program	Mar 1980
Instruction Report K-80-4	A Three-Dimensional Stability Analysis/Design Program (3DSAD)	
	Report 1:General Geometry Module	Jun 1980
	Report 3:General Analysis Module (CGAM)	Jun 1982
	Report 4:Special-Purpose Modules for Dams (CDAMS)	Aug 1983
Instruction Report K-80-6	Basic User's Guide:Computer Program for Design and Analysis of Inverted-T Retaining Walls and Floodwalls (TWDA)	Dec 1980
Instruction Report K-80-7	User's Reference Manual:Computer Program for Design and Analysis of Inverted-T Retaining Walls and Floodwalls (TWDA)	Dec 1980
Technical Report K-80-4	Documentation of Finite Element Analyses	
	Report 1:Longview Outlet Works Conduit	Dec 1980
	Report 2:Anchored Wall Monolith, Bay Springs Lock	Dec 1980
Technical Report K-80-5	Basic Pile Group Behavior	Dec 1980
Instruction Report K-81-2	User's Guide:Computer Program for Design and Analysis of Sheet Pile Walls by Classical Methods (CSHTWAL)	
	Report 1:Computational Processes	Feb 1981
	Report 2:Interactive Graphics Options	Mar 1981
Instruction Report K-81-3	Validation Report:Computer Program for Design and Analysis of Inverted-T Retaining Walls and Floodwalls (TWDA)	Feb 1981
Instruction Report K-81-4	User's Guide:Computer Program for Design and Analysis of Cast-in-Place Tunnel Linings (NEWTUN)	Mar 1981
Instruction Report K-81-6	User's Guide:Computer Program for Optimum Nonlinear Dynamic Design of Reinforced Concrete Slabs Under Blast Loading (CBARCS)	Mar 1981
Instruction Report K-81-7	User's Guide:Computer Program for Design or Investigation of Orthogonal Culverts (CORTCUL)	Mar 1981
Instruction Report K-81-9	User's Guide:Computer Program for Three-Dimensional Analysis of Building Systems (CTABS80)	Aug 1981
Technical Report K-81-2	Theoretical Basis for CTABS80:A Computer Program for Three-Dimensional Analysis of Building Systems	Sep 1981
Instruction Report K-82-6	User's Guide:Computer Program for Analysis of Beam-Column Structures with Nonlinear Supports (CBEAMC)	Jun 1982

(Continued)

WATERWAYS EXPERIMENT STATION REPORTS PUBLISHED UNDER THE COMPUTER-AIDED STRUCTURAL ENGINEERING (CASE) PROJECT

(Continued)

	Title	Date
Instruction Report K-82-7	User's Guide:Computer Program for Bearing Capacity Analysis of Shallow Foundations (CBEAR)	Jun 1982
Instruction Report K-83-1	User's Guide:Computer Program with Interactive Graphics for Analysis of Plane Frame Structures (CFRAME)	Jan 1983
Instruction Report K-83-2	User's Guide:Computer Program for Generation of Engineering Geometry (SKETCH)	Jun 1983
Instruction Report K-83-5	User's Guide:Computer Program to Calculate Shear, Moment, and Thrust (CSMT) from Stress Results of a Two-Dimensional Finite Element Analysis	Jul 1983
Technical Report K-83-1	Basic Pile Group Behavior	Sep 1983
Technical Report K-83-3	Reference Manual:Computer Graphics Program for Generation of Engineering Geometry (SKETCH)	Sep 1983
Technical Report K-83-4	Case Study of Six Major General-Purpose Finite Element Programs	Oct 1983
Instruction Report K-84-2	User's Guide:Computer Program for Optimum Dynamic Design of Nonlinear Metal Plates Under Blast Loading (CSDOOR)	Jan 1984
Instruction Report K-84-7	User's Guide:Computer Program for Determining Induced Stresses and Consolidation Settlements (CSETT)	Aug 1984
Instruction Report K-84-8	Seepage Analysis of Confined Flow Problems by the Method of Fragments (CFRAG)	Sep 1984
Instruction Report K-84-11	User's Guide for Computer Program CGFAG, Concrete General Flexure Analysis with Graphics	Sep 1984
Technical Report K-84-3	Computer-Aided Drafting and Design for Corps Structural Engineers	Oct 1984
Technical Report ATC-86-5	Decision Logic Table Formulation of ACI 318-77, Building Code Requirements for Reinforced Concrete for Automated Constraint Processing, Volumes I and II	Jun 1986
Technical Report ITL-87-2	A Case Committee Study of Finite Element Analysis of Concrete Flat Slabs	Jan 1987
Instruction Report ITL-87-1	User's Guide:Computer Program for Two-Dimensional Analysis of U-Frame Structures (CUFRAM)	Apr 1987
Instruction Report ITL-87-2	User's Guide:For Concrete Strength Investigation and Design (CASTR) in Accordance with ACI 318-83	May 1987
Technical Report ITL-87-6	Finite-Element Method Package for Solving Steady-State Seepage Problems	May 1987
Instruction Report ITL-87-3	User's Guide:A Three Dimensional Stability Analysis/Design Program (3DSAD) Module	Jun 1987
	Report 1:Revision 1:General Geometry	Jun 1987
	Report 2:General Loads Module	Sep 1989
	Report 6:Free-Body Module	Sep 1989

(Continued)

WATERWAYS EXPERIMENT STATION REPORTS PUBLISHED UNDER THE COMPUTER-AIDED STRUCTURAL ENGINEERING (CASE) PROJECT

(Continued)

	Title	Date
Instruction Report ITL-87-4	User's Guide:2-D Frame Analysis Link Program (LINK2D)	Jun 1987
Technical Report ITL-87-4	Finite Element Studies of a Horizontally Framed Miter Gate Report 1:Initial and Refined Finite Element Models (Phases A, B, and C), Volumes I and II Report 2:Simplified Frame Model (Phase D) Report 3:Alternate Configuration Miter Gate Finite Element Studies–Open Section Report 4:Alternate Configuration Miter Gate Finite Element Studies–Closed Sections Report 5:Alternate Configuration Miter Gate Finite Element Studies–Additional Closed Sections Report 6:Elastic Buckling of Girders in Horizontally Framed Miter Gates Report 7:Application and Summary	Aug 1987
Instruction Report GL-87-1	User's Guide:UTEXAS2 Slope-Stability Package; Volume I, User's Manual	Aug 1987
Instruction Report ITL-87-5	Sliding Stability of Concrete Structures (CSLIDE)	Oct 1987
Instruction Report ITL-87-6	Criteria Specifications for and Validation of a Computer Program for the Design or Investigation of Horizontally Framed Miter Gates (CMITER)	Dec 1987
Technical Report ITL-87-8	Procedure for Static Analysis of Gravity Dams Using the Finite Element Method – Phase 1a	Jan 1988
Instruction Report ITL-88-1	User's Guide:Computer Program for Analysis of Planar Grid Structures (CGRID)	Feb 1988
Technical Report ITL-88-1	Development of Design Formulas for Ribbed Mat Foundations on Expansive Soils	Apr 1988
Technical Report ITL-88-2	User's Guide:Pile Group Graphics Display (CPGG) Post-processor to CPGA Program	Apr 1988
Instruction Report ITL-88-2	User's Guide for Design and Investigation of Horizontally Framed Miter Gates (CMITER)	Jun 1988
Instruction Report ITL-88-4	User's Guide for Revised Computer Program to Calculate Shear, Moment, and Thrust (CSMT)	Sep 1988
Instruction Report GL-87-1	User's Guide:UTEXAS2 Slope-Stability Package; Volume II, Theory	Feb 1989
Technical Report ITL-89-3	User's Guide:Pile Group Analysis (CPGA) Computer Group	Jul 1989
Technical Report ITL-89-4	CBASIN–Structural Design of Saint Anthony Falls Stilling Basins According to Corps of Engineers Criteria for Hydraulic Structures; Computer Program X0098	Aug 1989

(Continued)

WATERWAYS EXPERIMENT STATION REPORTS PUBLISHED UNDER THE COMPUTER-AIDED STRUCTURAL ENGINEERING (CASE) PROJECT

(Continued)

	Title	Date
Technical Report ITL-89-5	CCHAN–Structural Design of Rectangular Channels According to Corps of Engineers Criteria for Hydraulic Structures; Computer Program X0097	Aug 1989
Technical Report ITL-89-6	The Response-Spectrum Dynamic Analysis of Gravity Dams Using the Finite Element Method; Phase II	Aug 1989
Contract Report ITL-89-1	State of the Art on Expert Systems Applications in Design, Construction, and Maintenance of Structures	Sep 1989
Instruction Report ITL-90-1	User's Guide:Computer Program for Design and Analysis of Sheet Pile Walls by Classical Methods (CWALSHT)	Feb 1990
Technical Report ITL-90-3	Investigation and Design of U-Frame Structures Using Program CUFRBC Volume A:Program Criteria and Documentation Volume B:User's Guide for Basins Volume C:User's Guide for Channels	May 1990
Instruction Report ITL-90-6	User's Guide:Computer Program for Two-Dimensional Analysis of U-Frame or W-Frame Structures (CWFRAM)	Sep 1990
Instruction Report ITL-90-2	User's Guide: Pile Group–Concrete Pile Analysis Program (CPGC) Preprocessor to CPGA Program	Jun 1990
Technical Report ITL-91-3	Application of Finite Element, Grid Generation, and Scientific Visualization Techniques to 2-D and 3-D Seepage and Groundwater Modeling	Sep 1990
Instruction Report ITL-91-1	User's Guide:Computer Program for Design and Analysis of Sheet-Pile Walls by Classical Methods (CWALSHT) Including Rowe's Moment Reduction	Oct 1991
Instruction Report ITL-87-2 (Revised)	User's Guide for Concrete Strength Investigation and Design (CASTR) in Accordance with ACI 318-89	Mar 1992
Technical Report ITL-92-2	Fiinite Element Modeling of Welded Thick Plates for Bonneville Navigation Lock	May 1992
Technical Report ITL-92-4	Introduction to the Computation of Response Spectrum for Earthquake Loading	Jun 1992
Instruction Report ITL-92-3	Concept Design Example, Computer Aided Structural Modeling (CASM) Report 1:Scheme A Report 2:Scheme B Report 3:Scheme C	 Jun 1992 Jun 1992 Jun 1992
Instruction Report ITL-92-4	User's Guide: Computer-Aided Structural Modeling (CASM) - Version 3.00	Apr 1992
Instruction Report ITL-92-5	Tutorial Guide: Computer-Aided Structural Modeling (CASM) - Version 3.00	Apr 1992

(Continued)

WATERWAYS EXPERIMENT STATION REPORTS PUBLISHED UNDER THE COMPUTER-AIDED STRUCTURAL ENGINEERING (CASE) PROJECT

(Continued)

	Title	Date
Contract Report ITL-92-1	Optimization of Steel Pile Foundations Using Optimality Criteria	Jun 1992
Technical Report ITL-92-7	Refined Stress Analysis of Melvin Price Locks and Dam	Sep 1992
Contract Report ITL-92-2	Knowledge-Based Expert System for Selection and Design of Retaining Structures	Sep 1992
Contract Report ITL-92-3	Evaluation of Thermal and Incremental Construction Effects for Monoliths AL-3 and AL-5 of the Melvin Price Locks and Dam	Sep 1992
Instruction Report GL-87-1	User's Guide:UTEXAS3 Slope-Stability Package; Volume IV, User's Manual	Nov 1992
Technical Report ITL-92-11	The Seismic Design of Waterfront Retaining Structures	Nov 1992
Technical Report ITL-92-12	Computer-Aided, Field-Verified Structural Evaluation	
	Report 1:Development of Computer Modeling Techniques for Miter Lock Gates	Nov 1992
	Report 2:Field Test and Analysis Correlation at John Hollis Bankhead Lock and Dam	Dec 1992
	Report 3:Field Test and Analysis Correlation of a Vertically Framed Miter Gate at Emsworth Lock and Dam	Dec 1993
Instruction Report GL-87-1	User's Guide:UTEXAS3 Slope-Stability Package; Volume III, Example Problems	Dec 1992
Technical Report ITL-93-1	Theoretical Manual for Analysis of Arch Dams	Jul 1993
Technical Report ITL-93-2	Steel Structures for Civil Works, General Considerations for Design and Rehabilitation	Aug 1993
Technical Report ITL-93-3	Soil-Structure Interaction Study of Red River Lock and Dam No. 1 Subjected to Sediment Loading	Sep 1993
Instruction Report ITL-93-3	User's Manual—ADAP, Graphics-Based Dam Analysis Program	Aug 1993
Instruction Report ITL-93-4	Load and Resistance Factor Design for Steel Miter Gates	Oct 1993
Technical Report ITL-94-2	User's Guide for the Incremental Construction, Soil-Structure Interaction Program SOILSTRUCT with Far-Field Boundary Elements	Mar 1994
Instruction Report ITL-94-1	Tutorial Guide: Computer-Aided Structural Modeling (CASM); Version 5.00	Apr 1994
Instruction Report ITL-94-2	User's Guide: Computer-Aided Structural Modeling (CASM); Version 5.00	Apr 1994
Technical Report ITL-94-4	Dynamics of Intake Towers and Other MDOF Structures Under Earthquake Loads: A Computer-Aided Approach	Jul 1994
Technical Report ITL-94-5	Procedure for Static Analysis of Gravity Dams Including Foundation Effects Using the Finite Element Method – Phase 1B	Jul 1994

(Continued)

WATERWAYS EXPERIMENT STATION REPORTS PUBLISHED UNDER THE COMPUTER-AIDED STRUCTURAL ENGINEERING (CASE) PROJECT

(Concluded)

	Title	Date
Instruction Report ITL-94-5	User's Guide: Computer Program for Winkler Soil-Structure Interaction Analysis of Sheet-Pile Walls (CWALSSI)	Nov 1994
Instruction Report ITL-94-6	User's Guide:Computer Program for Analysis of Beam-Column Structures with Nonlinear Supports (CBEAMC)	Nov 1994
Instruction Report ITL-94-7	User's Guide to CTWALL – A Microcomputer Program for the Analysis of Retaining and Flood Walls	Dec 1994
Contract Report ITL-95-1	Comparison of Barge Impact Experimental and Finite Element Results for the Lower Miter Gate of Lock and Dam 26	Jun 1995
Technical Report ITL-95-5	Soil-Structure Interaction Parameters for Structured/Cemented Silts	Aug 1995
Instruction Report ITL-95-1	User's Guide: Computer Program for the Design and Investigation of Horizontally Framed Miter Gates Using the Load and Resistance Factor Criteria (CMITER-LRFD)	Aug 1995
Technical Report ITL-95-8	Constitutive Modeling of Concrete for Massive Concrete Structures, A Simplified Overview	Sep 1995